horticulturae

MDPI

Article

Effects of Drought Stress on Leaf Micromorphology, Glandular Trichomes, and the Accumulation of Essential Oils and Flavonoids in Four Lamiaceae Species

Csilla Tóth [1], Enikő Bodó [2], Szabolcs Vigh [1] and Brigitta Tóth [2,3,*]

[1] Department of Agricultural Sciences and Environmental Management, Institute of Engineering and Agricultural Sciences, University of Nyíregyháza, Sóstói Str. 31/b, H-4400 Nyiregyhaza, Hungary; toth.csilla@nye.hu (C.T.); vigh.szabolcs@nye.hu (S.V.)

[2] Research and Innovation Center, University of Nyíregyháza, Sóstói Str. 31/b, H-4400 Nyiregyhaza, Hungary; bodo.eniko@nye.hu

[3] Institute of Food Science, Faculty of Agricultural and Food Sciences and Environmental Management, University of Debrecen, Böszörményi Str. 138, H-4032 Debrecen, Hungary

* Correspondence: btoth@agr.unideb.hu or toth.brigitta@nye.hu; Tel.: +36-30-2738842

Abstract

The effects of progressive drought stress were examined in four economically important plant species belonging to the Lamiaceae family: catnip (*Nepeta cataria* L.), lavender (*Lavandula angustifolia* Mill.), holy basil (*Ocimum tenuiflorum* L.), and perilla mint (*Perilla frutescens* (L.) Britton). Plants were grown in a controlled pot experiment under three soil water capacity levels: 70% (control), 50% (moderate stress), and 30% (severe stress), and the drought stress lasted for 30 days. The study evaluated a comprehensive set of leaf micromorphological parameters, including the density and diameter of glandular trichomes, stomatal density and size, and the thickness of the lamina, mesophyll, epidermis, cuticle, and parenchymal layers. In addition, essential oil (EO) content, total flavonoid content (TFC), and elemental composition were analyzed. Drought responses were strongly species-specific. *O. tenuiflorum*, *P. frutescens*, and *N. cataria* showed high sensitivity characterized by reduced biomass and thinning of leaf tissues. These changes were accompanied by typical xeromorphic adaptations, such as increased stomatal and glandular trichome density, and reduced stomatal size. *L. angustifolia* exhibited pronounced cuticle thickening, suggesting an effective structural mechanism to minimize water loss. Secondary metabolism also responded differently among species. In some cases, drought shifted metabolic allocation toward flavonoid accumulation at the expense of essential oils, whereas in others, moderate stress promoted the co-accumulation of both compounds. These patterns indicate distinct adaptive strategies linking anatomical plasticity with metabolic regulation. Overall, moderate drought supported adaptive responses, while severe water limitation impaired growth and metabolic production. From a practical perspective, maintaining moderate soil water availability appears critical to optimize both plant performance and the accumulation of valuable secondary metabolites in Lamiaceae species.

Keywords: ionomics; Lamiaceae; micromorphology; secondary metabolism; phenotypic plasticity; water deficit

Academic Editor: Francisco Garcia-Sanchez

Received: 17 March 2026
Revised: 8 April 2026
Accepted: 8 April 2026
Published: 10 April 2026

1. Introduction

The mint family (Lamiaceae) is one of the largest angiosperm families, comprising about 230–240 genera and over 7000 species worldwide. This makes it the sixth-largest angiosperm family and the largest within the order Lamiales [1,2]. Plants belonging to this family are widely used for the prevention and treatment of various human illnesses including diabetes, hypertension, flatulence, pulmonary infections, headaches, fever, cough, colds, urinary tract infections, gastric ulcers, epilepsy, bronchitis, asthma, and immunological disorders [3,4]. Numerous studies have highlighted the diverse therapeutic potential of different Lamiaceae genera, demonstrating antioxidant, antimicrobial, anti-inflammatory, antidiabetic, and cardioprotective properties [3–8].

Glandular trichomes are important epidermal structures in Lamiaceae leaves and play key ecological and physiological roles. They occur on both the adaxial and abaxial leaf surfaces and contribute to functions ranging from pollinator attraction to herbivore defence [9]. Morphologically, glandular trichomes are divided into two main types: capitate and peltate trichomes [10]. Capitate trichomes consist of a stalk and a small secretory head (10–30 μm in diameter) that mainly secretes polysaccharides along with a range of other metabolites [11–13]. In contrast, peltate trichomes have a short unicellular stalk and a large, multicellular secretory head (40–60 μm in diameter) [14–16]. These peltate glands represent the principal sites of essential oil accumulation, and their size and density are closely related to overall essential oil yield [17–19]. The development and activity of glandular trichomes are highly dynamic and strongly influenced by environmental conditions and seasonal changes [20–22].

Abiotic stresses, particularly drought, induce both anatomical and metabolic adaptations in plants. Moderate water deficit can stimulate the biosynthesis of essential oils and phenolic compounds as part of a protective antioxidant response, whereas severe drought often suppresses plant growth and metabolic activity [23–28]. As a result, water scarcity significantly alters biochemical profiles, often promoting the accumulation of bioactive compounds such as flavonoids, an important group of secondary metabolites with protective functions [29–31].

In addition to changes in trichome characteristics, plants adjust other microanatomical features under drought conditions. These include modifications in stomatal traits, cuticle thickness, and internal leaf structure, which collectively contribute to improved water-use efficiency and stress tolerance [32–37]. Typically, drought leads to smaller stomata and increased stomatal density, enabling more effective regulation of gas exchange and transpiration [38–40]. Leaves may also develop thicker epidermal layers and a more pronounced cuticle to reduce water loss [38,41].

Drought stress also affects nutrient uptake and ion homeostasis. Changes in the accumulation of macro- and microelements can influence metabolic processes, as many of these elements function as essential cofactors in secondary metabolite biosynthesis [42–49].

Despite the well-established relationship between environmental stress and secondary metabolism, the coordinated interactions among trichome morphology, stomatal traits, nutrient uptake, and metabolite accumulation under varying water availability remain insufficiently understood across Lamiaceae species.

To address this gap, the present study focuses on four economically important species with contrasting ecological origins and drought tolerance: *Nepeta cataria* L., *Lavandula angustifolia* Mill., *Ocimum tenuiflorum* L., and *Perilla frutescens* (L.) Britton. These species differ markedly in their adaptive strategies. *Lavandula angustifolia* Mill. (lavender), a Mediterranean xerophyte is well adapted to arid conditions and characterized by a thick cuticle and a predominance of peltate trichomes, which contribute to efficient water conservation and essential oil production [27,49,50]. In contrast, *Perilla frutescens* (L.) Britton

(perilla mint), native to humid environments, is more sensitive to water deficit, although drought can still influence its essential oil accumulation and trichome development [51,52]. *Ocimum tenuiflorum* L. (holy basil) exhibits intermediate drought tolerance and responds to water stress with adjustments in both essential oil production and glandular trichome density [24,25,33,53]. *Nepeta cataria* L. (catnip), a temperate species with relatively broad ecological adaptability, shows moderate to high drought tolerance and maintains active secondary metabolism under stress conditions [17,23,54,55].

Unlike previous studies that have examined these traits individually, this approach allows a more integrated evaluation of anatomical, ionomic, and photochemical responses across multiple species. By comparing these specific the study provides a framework for understanding how contrasting ecological backgrounds influence the coordination of structural and metabolic responses to drought stress. The objective of this study was to investigate how different soil water capacity levels (70%, 50%, and 30% SWC) affect leaf microanatomy (size and density of glandular trichomes and stomata), elemental composition, and secondary metabolite production in four selected Lamiaceae species (*L. angustifolia*, *P. frutescens*, *O. tenuiflorum*, and *N. cataria*). Microanatomical traits were analyzed in all four species, while elemental and physiological measurements were evaluated in three species (L. angustifolia, O. tenuiflorum, and *N. cataria*) due to limited sample availability of *P. frutescens* under severe drought conditions. The selected soil water capacity levels (70%, 50%, and 30% SWC) were chosen to represent well-watered conditions, moderate drought stress, and severe drought stress, respectively, following commonly applied thresholds in controlled drought experiments for medicinal and aromatic plants. We hypothesized that: (i) moderate drought stress increases glandular trichome development and promotes the accumulation of essential oils and flavonoids; (ii) severe drought stress limits both microanatomical development and biosynthetic activity; and (iii) these responses are species specific, reflecting diverse drought tolerance strategies. By integrating micromorphological, ionomic, and phytochemical traits, this study provides a comprehensive understanding of drought adaptation in Lamiaceae species.

2. Materials and Methods

2.1. Plant Material and Experimental Design

A controlled pot experiment was conducted to evaluate drought responses in four Lamiaceae species: holy basil (*Ocimum tenuiflorum* L.), perilla mint (*Perilla frutescens* (L.) Britton), catnip (*Nepeta cataria* L.), and lavender (*Lavandula angustifolia* Mill.). Plants were exposed to three soil water capacity (SWC) levels: 70% (well-watered control), 50% (moderate drought stress), and 30% (severe drought stress).

Certified seeds of *Nepeta cataria* L. and *Lavandula angustifolia* Mill. were supplied by Rédei Kertimag Zrt. (Réde, Hungary), whereas seeds of *Ocimum tenuiflorum* L. and *Perilla frutescens* (L.) Britton were obtained from Rocalba S.A. (Linares, Spain) and Legutko Invest Sp.J. (Jutrosin, Poland), respectively. Seeds were sown in seedling trays (39 cm × 11 cm × 25 cm) in early April 2025. Seedlings were cultivated in a controlled-environment growth chamber at the Department of Engineering and Agricultural Sciences, University of Nyíregyháza, under a 16/8 h light/dark photoperiod at 25/19 °C (day/night), 60% relative humidity, and a photosynthetic photon flux density (PPFD) of 300 µmol m^{-2} s^{-1}.

Two-month-old seedlings were transplanted into pots with a diameter of 20 cm. Each pot was filled with 5 kg of a mixture of sandy loam and peat moss (1:1, *v*/*v*). One plant per pot was established, with 10 replicates per treatment for each species.

After transplanting, the pots were transferred to a greenhouse at the Research Institute of Nyíregyháza, Institutes for Agricultural Research and Educational Farm, University of Debrecen (Westsik Experimental Station, Nyíregyháza, Hungary). The experiment

was arranged in a randomized block design. Pots were maintained under greenhouse conditions to exclude natural precipitation. The average temperature inside the greenhouse during the experimental period was 25.1 °C. Drought stress treatments were initiated four weeks after transplanting and maintained for 30 days. No fertilizers or pesticides were applied during the experiment.

2.2. Growing Medium and Soil Characteristics

The sandy loam used in the soil media mixture was sourced from the Demonstration Garden of the University of Nyíregyháza (47.9737° N, 21.7089° E), located in Nyíregyháza, Szabolcs-Szatmár-Bereg County, Hungary. The basic characteristics of the soil mixture were as follows: pH(KCl): 7.11; total soluble salt < 0.02% (m/m); CaCO3 (m m^{-1}%): <0.1; humus (m m^{-1}%): 3.09%; NO_2-N—NO_3-N: 38.29; SO_4^{2-}: 298; P_2O_5: 274, K_2O: 281, Na: 36.1; Mg: 146.7; Cu: 2.05, Mn: 41.81, and Zn: 6.77 mg kg^{-1}. Analyses were performed in accordance with Hungarian Standard MSZ-08–0210:1977, MSZ-08–0206-2:1978, MSZ-08–0458:1980, and Standard MSZ 20135:1999 [56–59].

Soil water capacity (SWC) levels were defined as percentages of field capacity (FC), which was determined gravimetrically using a modified method according to Reynolds [60]. The substrate was saturated with water and allowed to drain freely for 24 h, after which the weight corresponding to field capacity (WFC) was recorded. The oven-dry weight (WD) was determined after drying at 105 °C to constant mass was achieved. Target pot weights corresponding to 70%, 50%, and 30% SWC were calculated based on the difference between WFC and WD using the following equation:

$$SWC(\%) = \frac{WC - WD}{WFC - WD} \times 100$$

where WC represents the actual pot weight at the time of measurement.

Three irrigation regimes were applied: 70% FC (well-watered control), 50% FC (moderate drought stress), and 30% FC (severe drought stress). Soil moisture was monitored daily by weighing each pot, and water was added as needed to maintain the predefined SWC levels. Irrigation was performed daily at a fixed time (09:00 a.m.). Target weights were adjusted weekly to account for increasing plant biomass.

The drought stress treatments were maintained for 30 days. At the end of the experimental period, plant samples were harvested.

2.3. Micromorphological Analysis

Microanatomical investigations were conducted on all four species (*N. cataria*, *L. angustifolia*, *O. tenuiflorum*, *P. frutescens*) to compare glandular trichome density and leaf micromorphology; however, phytochemical analyses (essential oil and total flavonoid content) were performed only for *N. cataria*, *L. angustifolia*, and *O. tenuiflorum*. In *P. frutescens*, severe structural degradation and reduced biomass under drought conditions limited the availability of suitable plant material for reliable phytochemical determination.

Leaf samples for microanatomical examinations were collected at the end of the experimental period, coinciding with the flowering stage. Ten healthy, fully developed leaves were harvested from the third internode, counted from the apex, of each plant. The collected leaves were preserved in Strasburger–Flemming solution (a mixture of 96% ethanol, 99.5% glycerol, and distilled water in a 1:1:1 v/v ratio [61]) until sectioning and preparation of epidermal imprints.

Epidermal imprints were prepared from leaf samples following the methods of Hilu and Randall [62], Gardner et al. [63], and Elagöz et al. [64]. Clear nail polish was applied to both the adaxial and abaxial surfaces of the leaves. After drying, the resulting films

were carefully peeled off and mounted on glass slides. The imprints were examined using an Olympus BX51 light microscope (Olympus Corporation, Tokyo, Japan). The following micromorphological parameters were evaluated on both adaxial and abaxial epidermal imprints: stomatal length (µm), stomatal width (µm), and stomatal density (no. mm^{-2}).

To examine glandular trichome characteristics, the method of García-Gutiérrez et al. [65] was employed. Leaf segments from the middle part of the lamina were partially digested in Franklin's solution (a mixture of 35% hydrogen peroxide and glacial acetic acid in a 1:1 v/v ratio) at room temperature for 24 h. After washing with distilled water, the samples were cleared in a sodium hypochlorite solution (25–50% in water) to render the epidermis transparent and subsequently stained with a 0.01% aqueous safranin solution (Merck KGaA, Darmstadt, Germany). The following micromorphometric parameters were evaluated on both adaxial and abaxial epidermal surfaces: density of capitate glandular trichomes (no. mm^{-2}), density of peltate glandular trichomes (no. mm^{-2}), and diameter of peltate glandular trichomes (µm) using an Olympus BX51 light microscope.

For further micromorphological analysis of the abaxial leaf surface, a Keyence WHX EA-300 digital microscope (Keyence Corp. of America, Itasca, IL, USA) was used. Three plants per treatment were selected for analysis. Ten leaf discs (5 mm in diameter) per plant were excised from the central part of the leaf blade and fixed in Strasburger–Flemming solution. Peltate glandular trichome density was determined by counting the number of trichomes within a defined area (1 mm^2). Three regions per sample were analyzed, with ten replicates per plant, following the modified method of Radácsi et al. [66]. Additionally, the diameter of peltate glandular trichomes was measured on ten randomly selected, intact trichomes per sample [24].

Leaf cross-sections were prepared from the middle third of the lamina using razor blades, following the method of Sass [67]. The sections were examined using an Olympus BX51 light microscope (Olympus Corporation, Tokyo, Japan) and stained with a 0.01% aqueous safranin solution (Merck KGaA, Darmstadt, Germany). The following micromorphometric parameters were measured: thickness of the lamina, mesophyll, adaxial and abaxial epidermis, adaxial and abaxial cuticle, as well as palisade and spongy parenchyma (all in µm). Digital images were captured using a VSI RZ302 3M CMOS camera (Beijing BestScope Technology Co., Ltd., Beijing, China), and measurements were performed using the VSI RZ302 software. Cross-sections and epidermal imprints were documented at total magnifications of 40×, 100×, 200×, and 400× (corresponding to 4×, 10×, 20×, and 40× objectives). All parameters were measured in 10 replicates per sample, and the values were averaged.

2.4. Biochemical Analyses

Relative water content (RWC) was determined using fully expanded young leaves collected from three plants per treatment for each species. Leaves were harvested from the fourth internode, counting from the shoot apex. The fresh mass (FM) was recorded immediately after sampling. Subsequently, the leaves were rehydrated in distilled water for 24 h to reach full turgor. After rehydration, surface moisture was gently removed with tissue paper, and the turgid mass (TM) was measured. Finally, samples were oven-dried at 35 °C for 72 h until constant weight was achieved, and the dry mass (DM). RWC was calculated using the following equation [68,69]:

$$RWC = \frac{FM - DM}{TM - DM} \times 100$$

For the determination of total flavonoid content (TFC), 10 g of dried leaves from *Nepeta cataria*, *Lavandula angustifolia*, and *Ocimum tenuiflorum* were extracted with 200 mL

of boiling distilled water for 30 min using a magnetic stirrer. The resulting primary extracts were allowed to cool to room temperature, filtered, and stored at 4 °C until analysis.

Total flavonoid content was determined using the aluminum chloride colorimetric method according to Kim et al. [70]. The reagent solution was prepared by dissolving 0.5 g of aluminum chloride ($AlCl_3$, Sigma, London, UK) and 0.41 g of potassium acetate (CH_3COOK, Sigma, London, UK) in a mixture of 150 mL of distilled water and 75 mL of methanol.

For the measurement, 0.5 mL of each plant extract was mixed with 4.5 mL of the reagent solution. The mixture was filtered through a 0.45 µm membrane filter, and the absorbance was measured at 415 nm using a PerkinElmer Lambda 35 spectrophotometer (PerkinElmer, Inc., Waltham, MA, USA). All measurements were performed in triplicate. Total flavonoid contents were calculated using a calibration curve prepared with rutin (10–200 µg mL^{-1}), and results were expressed as milligrams of rutin equivalents per gram (mg RE g^{-1} DW).

2.5. Essential Oil Content Determination

To determine the essential oil (EO) content, five plants per treatment were harvested and oven-dried at 30 °C until constant weight was achieved. The dried leaves and inflorescences were separated from the stems, ground into a fine powder, and passed through a 0.5 mm sieve. For each sample, 30 g of dried material was subjected to hydrodistillation for 2 h using a Clevenger-type apparatus (Sigma, London, UK) with 500 mL of distilled water. The extraction was performed in triplicate. The EO content was calculated based on the dry weight (DW) basis and expressed as mL 100 g^{-1} DW, following the guidelines of the VII Hungarian Pharmacopoeia [71].

2.6. Element Content Determination

Elemental composition was determined for three species (*Nepeta cataria*, *Lavandula angustifolia*, and *Ocimum tenuiflorum*). Due to the severe structural degradation and strongly reduced biomass observed in Perilla frutescens under drought stress, sufficient plant material for reliable elemental analysis was not available; therefore, this species was excluded from the ionomic evaluation.

For elemental analysis, 1 g samples of shoot and leaves were collected and dried at 60 °C for 48 h. The dried material was subject to a digestion procedure before analysis. Pre-digestion was initiated by adding concentrated H_2O_2 (Sigma, London, UK) to the sample-containing flask and allowing it to react for 1 h. Subsequently, concentrated HNO_3 (Sigma, London, UK) was added, and the mixture was heated at 60 °C for 15 min, followed by further digestion at 120 °C for 45 min. After digestion, the solutions were allowed to cool off and diluted with distilled water to a final volume of 50 cm^3. The resulting solutions were homogenized and filtered through MN 640 W filter paper (Macherey-Nagel, Düren, Germany). Elemental concentrations in the filtrates were determined using an inductively coupled plasma–optical emission spectrometer (ICP-OES; Spectro Genesis, SPECTRO, Freital, Germany). Calibration was performed using a multi-element standard solution containing all the measured elements (Loba Chemie Product code: I166N, Loba Chemie PVT, Mumbai, India). All samples were prepared and analyzed in triplicate.

2.7. Statistical Analysis

The pot containing a single plant represented the experimental unit. For anatomical measurements, multiple technical replicates were obtained from each biological replicate (plant), while biochemical and elemental analyses were conducted using independent biological replicates depending on the availability of plant material.

Data normality was assessed using the Shapiro–Wilk test. As the datasets for essential oil (EO) content, total flavonoid content (TFC), elemental composition, and micromorphometric parameters were normally distributed, parametric tests were applied. To evaluate the effects of plant species, drought-stress treatments, and their interaction on microanatomical parameters and elemental composition, a two-way analysis of variance (ANOVA) was performed. Differences among the three soil water capacity (SWC) treatment levels (70%, 50%, and 30%) within each species were analyzed using one-way ANOVA, followed by Tukey's HSD post hoc test for multiple comparisons ($p < 0.05$). Pearson's correlation coefficients (r) were calculated to examine relationships among soil water capacity (SWC), EO content, TFC, relative water content (RWC), dry weight (DW), elemental composition, and the measured micromorphometric traits, including the size and density of peltate glandular trichomes. Statistical analyses were primarily conducted using IBM SPSS Statistics 26 (IBM Corp., Armonk, NY, USA). Figure preparation and selected ANOVA analyses were performed using GraphPad Prism 11.0.0 (GraphPad Software, Boston, MA, USA). In figures and tables, different lowercase letters indicate statistically significant differences between treatments within the same species according to Tukey's HSD post hoc test ($p < 0.05$).

3. Results

3.1. Biomass, Relative Water Content, Essential Oil Yield, and Flavonoid Accumulation

Water supply significantly influenced the relative water content (RWC) and secondary metabolite accumulation (essential oil and total flavonoid content) in all examined species (Figure 1). RWC declined under drought conditions in all species, with the strongest reduction observed under severe stress. This decrease was most pronounced in *N. cataria* (19.7%), while *O. tenuiflorum* and *L. angustifolia* showed smaller but still significant reduction (16.6% and 14.2, respectively) (Figure 1A).

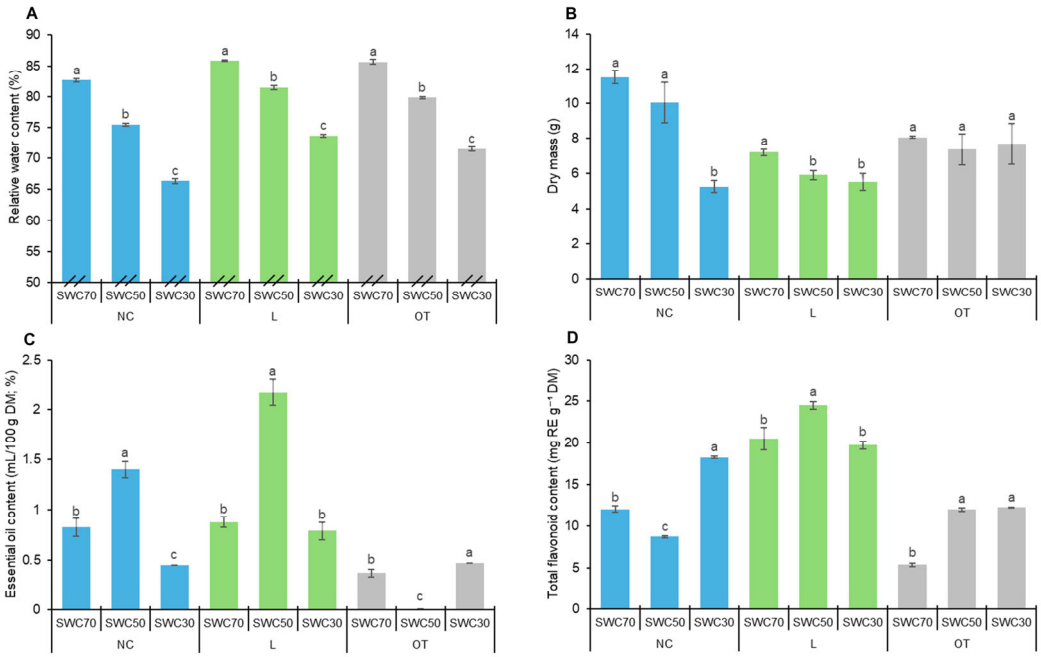

Figure 1. Effect of different soil water capacities (SWC70, SWC50, and SWC30) on leaf relative water content (%) (**A**), shoot dry mass (g plant^{-1}) (**B**), essential oil content (mL 100 g^{-1} DM; %) (**C**), and total flavonoid content (mg RE g^{-1} DM) (**D**) of *Nepeta cataria* (NC), *Lavandula angustifolia* (L), and *Ocimum tenuiflorum* (OT). Data represent the mean ± SD ($n = 3$). Different lowercase letters indicate significant differences between treatments within the same species according to Tukey's HSD post hoc test ($p < 0.05$).

Biomass accumulation (Figure 1B) was also strongly affected by drought and differed among species. *N. cataria* was the most sensitive, showing a 54.34% reduction in dry mass under severe drought compared to the control. *L. angustifolia* also exhibited a decrease in biomass, although less pronounced, whereas *O. tenuiflorum* maintained relatively stable biomass across treatments.

Essential oil (EO) yield showed clear species-specific responses to water deficit (Figure 1C). In *N. cataria*, EO content increased under moderate drought but declined sharply under severe stress, falling by 45.8% relative to the control. *L. angustifolia* exhibited maximum EO accumulation under moderate drought, whereas *O. tenuiflorum* showed the highest EO content under severe drought, where it increased by 27% compared to the control.

Total flavonoids (TFC) also displayed distinct patterns among species (Figure 1D). In *N. cataria*, TFC decreased under moderate drought but increased under severe stress, reaching values 50.9% higher than in the control. *L. angustifolia* showed peak flavonoid accumulation under moderate drought, while *O. tenuiflorum* exhibited consistently elevated TFC under both moderate and severe stress, with increases exceeding 120% relative to the well-watered treatment.

3.2. Leaf Micromorphological Parameters and Glandular Trichome Density

Tukey's post hoc analysis revealed significant species-specific anatomical responses to decreasing soil water capacity (Table 1).

3.2.1. Leaf Structural Traits

Leaf blade and mesophyll thickness showed a consistent response to drought intensity (Figures 2–5). Under moderate water deficit (50% SWC), these parameters generally increased in *N. cataria*, *L. angustifolis*, and *O. tenuiflorum*. In contrast, severe drought (30% SWC) reduced both traits to or below control levels. The strongest reductions were observed in *P. frutescens*, where leaf blade and mesophyll thickness decreased by 16.8% and 22.1%, respectively.

A similar trend was observed for palisade parenchyma thickness, which declined under severe drought in all species, particularly in *O. tenuiflorum* (−31.2%) and *P. frutescens* (−20.4%).

Cuticle thickness increased markedly under drought conditions, especially under severe stress. This response was most pronounced in *L. angustifolia*, where adaxial cuticle thickness increased by 170.34% compared to the control. Substantial increases were also observed in *N. cataria* (up to 117.9%), while *O. tenuiflorum* showed more moderate changes. In contrast, *P. frutescens* exhibited no significant change in adaxial cuticle thickness and a decrease on the abaxial surface.

Epidermal thickness showed contrasting patterns among species. Under severe drought, adaxial epidermal thickness decreased in *N. cataria*, *L. angustifolia*, and *O. tenuiflorum* (by 31.6%, 19.7%, and 33.5%, respectively), whereas *P. frutescens* exhibited an increase of approximately 45%. Changes in the abaxial epidermis were less pronounced, with significant differences observed only in *N. cataria*.

3.2.2. Glandular Trichome Characteristics

Glandular trichome density was strongly affected by drought (Figures 2–5). In general, both capitate and peltate trichomes increased under water deficit, particularly under moderate stress. In *P. frutescens* and *O. tenuiflorum*, adaxial capitate trichome density increased markedly, reaching approximately 2.6–2.9-fold higher values compared to the control. However, in *P. frutescens*, severe drought caused reduced capitate trichome density relative to moderate stress.

Table 1. Effects of three soil water capacity levels (SWC 70%, SWC 50%, and SWC 30%) on leaf microanatomical characteristics of *Nepeta cataria* L., *Lavandula angustifolia* Mill., *Ocimum tenuiflorum* L., and *Perilla frutescens* (L.) Britton.

Parameter	Treatment	*N. cataria*	*L. angustifolia*	*O. tenuiflorum*	*P. frutescens*
Lamina thickness (µm)	SWC 70%	101.34 ± 3.342 ab	339.41 ± 18.45 b	279.89 ± 4.12 b	119.65 ± 18.37 a
	SWC 50%	129.14 ± 46.43 a	363.89 ± 10.45 a	290.96 ± 6.15 a	117.57 ± 6.48 a
	SWC 30%	96.24 ± 4.62 b	322.81 ± 13.60 c	279.98 ± 9.64 b	99.55 ± 3.78 b
Mesophyll thickness (µm)	SWC 70%	70.79 ± 3.36 b	276.12 ± 3.56 b	241.59 ± 9.67 b	85.77 ± 10.03 b
	SWC 50%	80.28 ± 1.75 a	295.17 ± 9.77 a	280.03 ± 21.08 a	111.83 ± 7.78 a
	SWC 30%	62.19 ± 2.43 c	260.69 ± 6.61 c	238.96 ± 12.21 b	66.84 ± 1.48 c
Adaxial cuticle (µm)	SWC 70%	1.45 ± 0.26 b	1.45 ± 0.18 c	1.52 ± 0.26 a	1.57 ± 0.23 b
	SWC 50%	1.45 ± 0.26 b	2.8 ± 0.56 b	1.79 ± 0.60 a	1.85 ± 0.25 a
	SWC 30%	3.16 ± 1.00 a	3.92 ± 1.10 a	1.90 ± 0.62 a	1.53 ± 0.08 b
Adaxial epidermis (µm)	SWC 70%	18.23 ± 3.47 a	30.73 ± 2.59 a	26.66 ± 4.09 a	12.43 ± 1.94 b
	SWC 50%	16.34 ± 3.14 ab	27.64 ± 2.59 ab	23.32 ± 7.41 ab	16.42 ± 4.61 ab
	SWC 30%	12.47 ± 3.93 b	24.68 ± 2.49 b	17.85 ± 3.18 b	18.07 ± 3.14 a
Palisade parenchyma (µm)	SWC 70%	30.77 ± 2.93 b	129.03 ± 7.37 a	128.14 ± 7.84 a	53.56 ± 5.74 a
	SWC 50%	34.99 ± 3.54 a	130.13 ± 3.45 a	131.31 ± 17.60 a	50.65 ± 4.19 a
	SWC 30%	32.41 ± 2.26 ab	102.72 ± 9.93 b	88.13 ± 6.83 b	29.41 ± 3.93 b
Spongy parenchyma (µm)	SWC 70%	40.59 ± 3.75 b	116.32 ± 7.02 b	139.96 ± 7.97 a	46.78 ±6.47 b
	SWC 50%	44.98 ± 3.11 a	143.47 ± 8.89 a	148.71 ± 8.64 a	53.55 ±3.49 a
	SWC 30%	39.43 ± 3.41 b	113.39 ± 8.72 b	141.91 ± 7.81 a	40.17 ±3.57 c
Abaxial epidermis (µm)	SWC 70%	11.06 ± 1.98 b	14.96 ± 3.31 a	16.12 ± 4.72 a	15.76 ± 3.23 a
	SWC 50%	13.34 ± 1.54 a	14.26 ± 3.31 a	16.67 ± 4.42 a	14.24 ± 1.60 a
	SWC 30%	9.05 ± 0.58 c	13.18 ± 2.72 a	16.97 ± 4.09 a	15.78 ± 1.94 a
Abaxial cuticle (µm)	SWC 70%	1.09 ± 0.29716 b	2.25 ± 0.48 b	1.67 ± 0.34 b	1.66 ± 0.20 a
	SWC 50%	1.51 ± 0.47958 b	2.32 ± 0.39 b	1.82 ± 0.59 ab	1.32 ± 0.14 b
	SWC 30%	2.09 ± 0.65917 a	4.33 ± 0.73 a	2.33 ± 0.65 a	1.39 ± 0.10 b
AdCGT-D (no. mm^{-2})	SWC 70%	99 ± 13.61 a	1.2 ± 0.44 a	15.8 ± 2.28 b	8.2 ± 2.68 b
	SWC 50%	116 ± 13.46 a	1.4 ± 0.54 a	40.8 ± 11.09 a	23.4 ± 6.54 a
	SWC 30%	123 ± 16.77 a	1.4 ± 0.54 a	44 ± 7.48 a	14 ± 2.64 b
AdPGT-D (no. mm^{-2})	SWC 70%	1.2 ± 0.08 b	1.4 ± 0.54 c	0.8 ± 0.33 b	0
	SWC 50%	2.3 ± 0.38 a	2.8 ± 0.84 b	2.72 ± 0.76 a	0
	SWC 30%	1.4 ± 0.23 b	4.4 ± 0.89 a	2.8 ± 0.4 a	0
AdPGT-Dia (µm)	SWC 70%	58.41 ± 6.62 a	78.48 ± 6.96 a	63.53 ± 12.01 b	n. a.
	SWC 50%	46.17 ± 6.67 b	78.22 ± 5.38 a	72.03 ± 4.37 ab	n. a.
	SWC 30%	54.72 ± 6.99 a	82.82 ± 3.77 a	75.15 ± 7.18 a	n. a.
AbCGT-D (no. mm^{-2})	SWC 70%	120 ± 16 a	2.2 ± 0.44 a	75.2 ± 26.14 a	6.2 ± 2.86 b
	SWC 50%	60 ± 27.32 b	2.4 ± 0.54 a	44 ± 9.38 b	20.4 ± 3.84 a
	SWC 30%	60 ± 20.13 b	2.6 ± 0.54 a	44.8 ± 3.34 b	18.6 ± 2.07 a
AbPGT-D (no. mm^{-2})	SWC 70%	3.84 ± 1.43 b	7.82 ± 1.06 a	2.83 ± 0.33 a	0.39 ± 0.21 a
	SWC 50%	9.32 ± 0.71 a	5.91 ± 1.07 a	3.6 ± 0.57 a	0.94 ± 0.31 a
	SWC 30%	3.25 ± 0.75 b	8.18 ± 1.01 a	3.54 ± 0.46 a	0.44 ± 0.29 a
AbPGT-Dia (µm)	SWC 70%	71.94 ± 0.86 a	86.82 ± 0.74 a	87.89 ± 3.69 a	70.82 ± 1.86 a
	SWC 50%	62.91 ± 1.92 b	81.75 ± 2.41 b	80.82 ± 3.06 a	70.82 ± 1.19 a
	SWC 30%	70.08 ± 2.82 a	86.34 ± 1.27 a	83.04 ± 1.23 a	72.84 ± 0.05 a

Data represent the mean of ten replicates ± SD. Different lowercase letters within a column for a given parameter indicate statistically significant differences between water treatments at $p < 0.05$ (ANOVA followed by Tukey's HSD post hoc test). n.a.: not applicable (due to the absence of peltate trichomes); AdCGT-D: number of capitate glandular trichomes (no. mm^{-2}) in adaxial epidermis; AdPGT-D: number of peltate glandular trichomes (no. mm^{-2}) in adaxial epidermis; AdPGT-Dia: diameter of peltate glandular trichomes (µm) on adaxial epidermis; AbCGT-D: number of capitate glandular trichomes (no. mm^{-2}) in abaxial epidermis; AbPGT-D: number of peltate glandular trichomes (no. mm^{-2}) in abaxial epidermis; AbPGT-Dia: diameter of peltate glandular trichomes (µm) in abaxial epidermis.

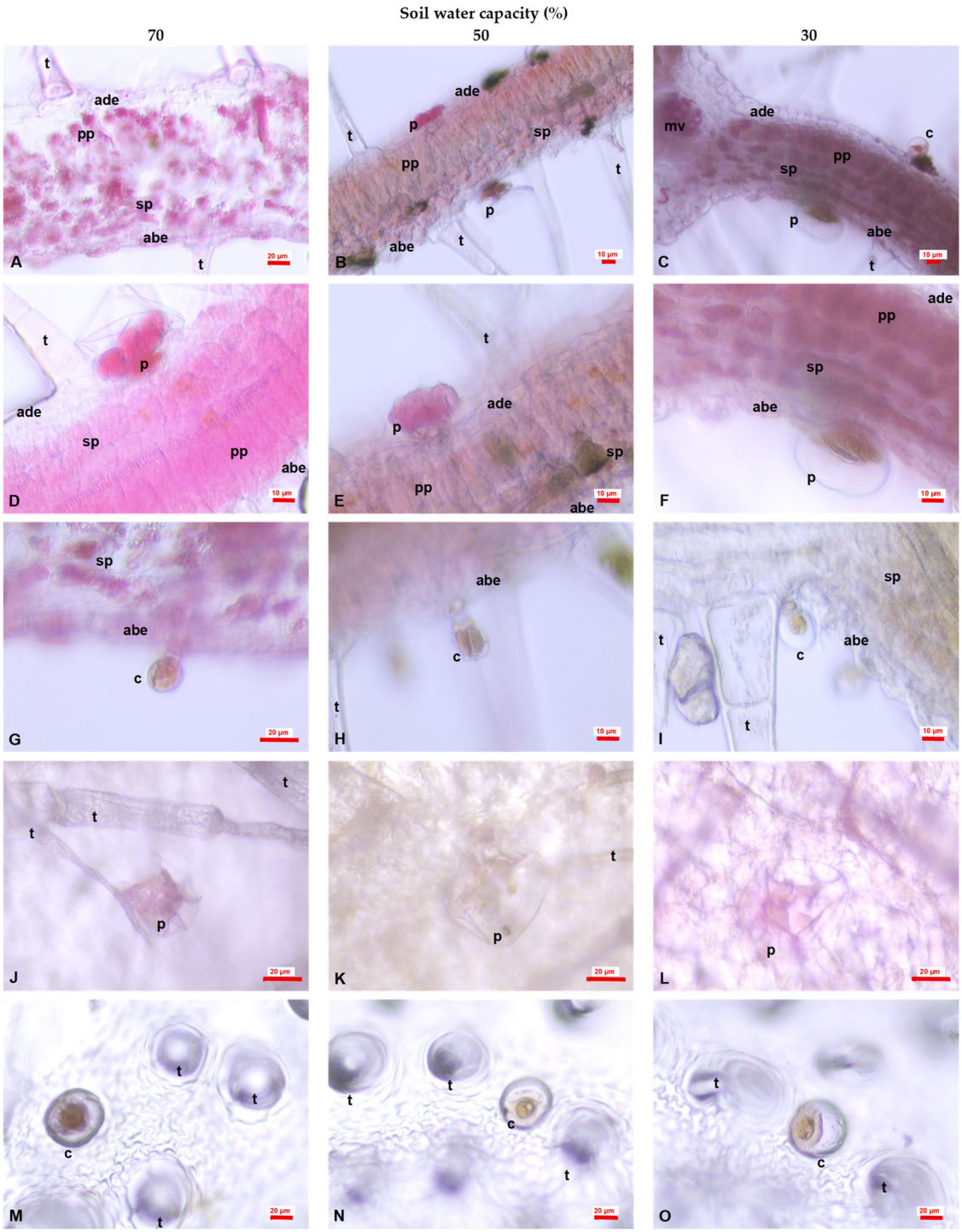

Figure 2. Effects of three soil water capacity levels (SWC70, SWC50, and SWC30) on leaf microanatomical characteristics of *Nepeta cataria* L. (**A**–**C**) Transverse sections of leaf laminae showing leaf mesophyll (20×); scale bars: 10, 20 µm. (**D**–**F**) Peltate glandular trichomes with multicellular secretory head (40×); scale bars: 10 µm. (**G**) Capitate glandular trichome with unicellular head and unicellular stalk (40×); scale bars: 20 µm. (**H**,**I**) Capitate glandular trichomes with bicellular head and unicellular stalk (40×); scale bars: 10 µm. (**J**–**L**) Peltate glandular trichomes on abaxial epidermis layer (40×); scale bars: 20 µm. (**M**–**O**) Capitate glandular trichomes with visible oil droplet on adaxial epidermis layer (40×); scale bars: 20 µm. abe: abaxial epidermis; ade: adaxial epidermis; c: capitate glandular trichomes; p: peltate glandular trichomes; pp: palisade parenchyma; sp: spongy parenchyma; t: non-glandular trichomes; mv: main vein.

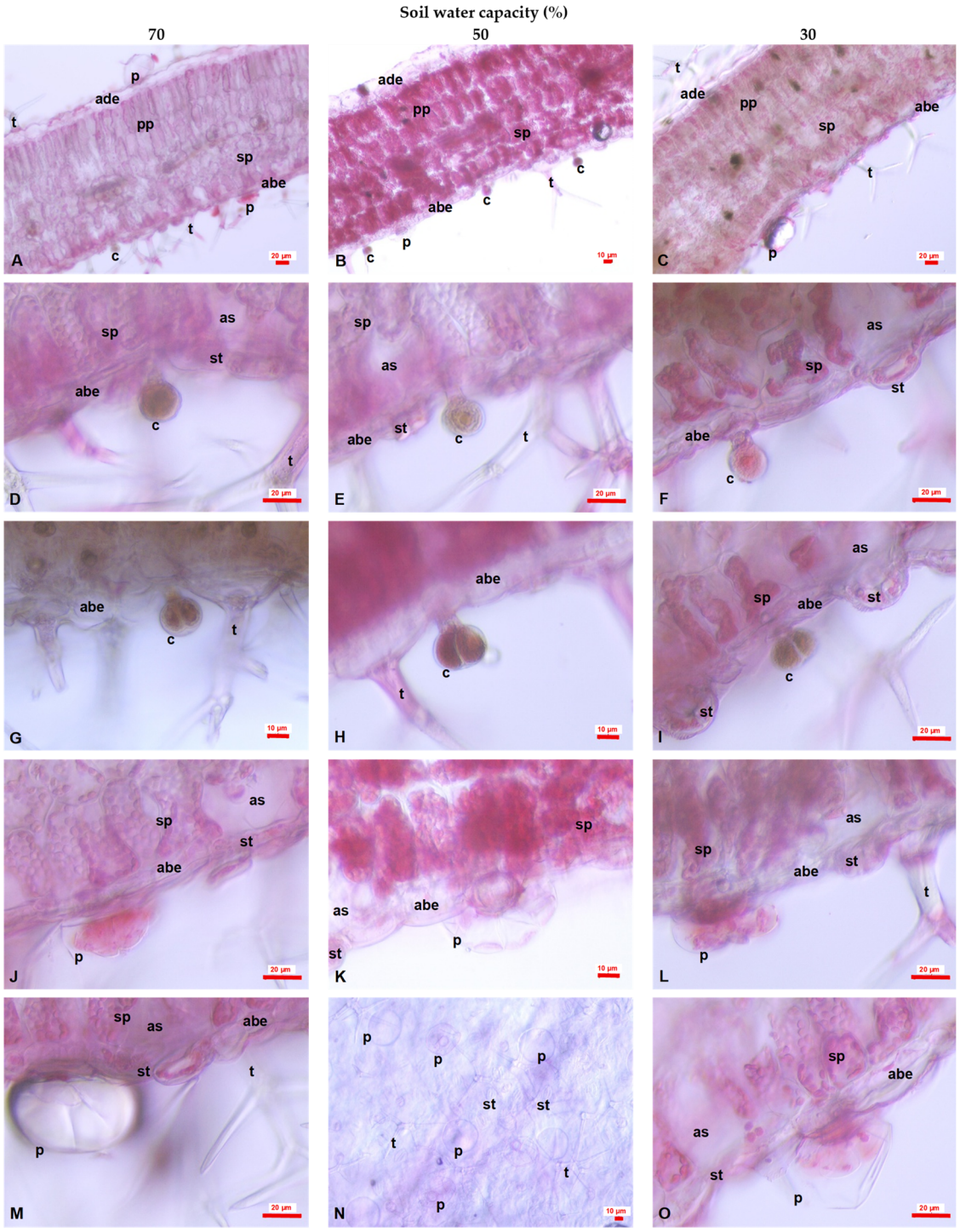

Figure 3. Effects of three different soil water capacity levels (SWC70, SWC50, and SWC30) on leaf microanatomical characteristics of *Lavandula angustifolia* Mill. (**A**–**C**) Transverse sections of leaf laminae showing leaf mesophyll (20×); scale bars: 10, 20 µm. (**D**–**F**) Capitate glandular trichomes with unicellular head and unicellular stalk (40×); scale bars: 20 µm. (**G**–**I**) Capitate glandular trichomes with bicellular head and unicellular stalk (20×); scale bars: 10, 20 µm. (**J**–**L**) Peltate glandular trichomes showing round multicellular secretory head and short unicellular stalk (40×); scale bars: 10, 20 µm. (**M**) Peltate glandular trichomes (40×); scale bars: 20 µm. (**N**) Peltate glandular trichomes and non-glandular trichomes in the abaxial epidermis layer (20×); scale bars: 10 µm. (**O**) Peltate glandular trichomes (40×); scale bars: 20 µm. abe: abaxial epidermis; ade: adaxial epidermis; as: air space; c: capitate glandular trichomes; p: peltate glandular trichomes; pp: palisade parenchyma; sp: spongy parenchyma; st: stomata; t: non-glandular trichomes.

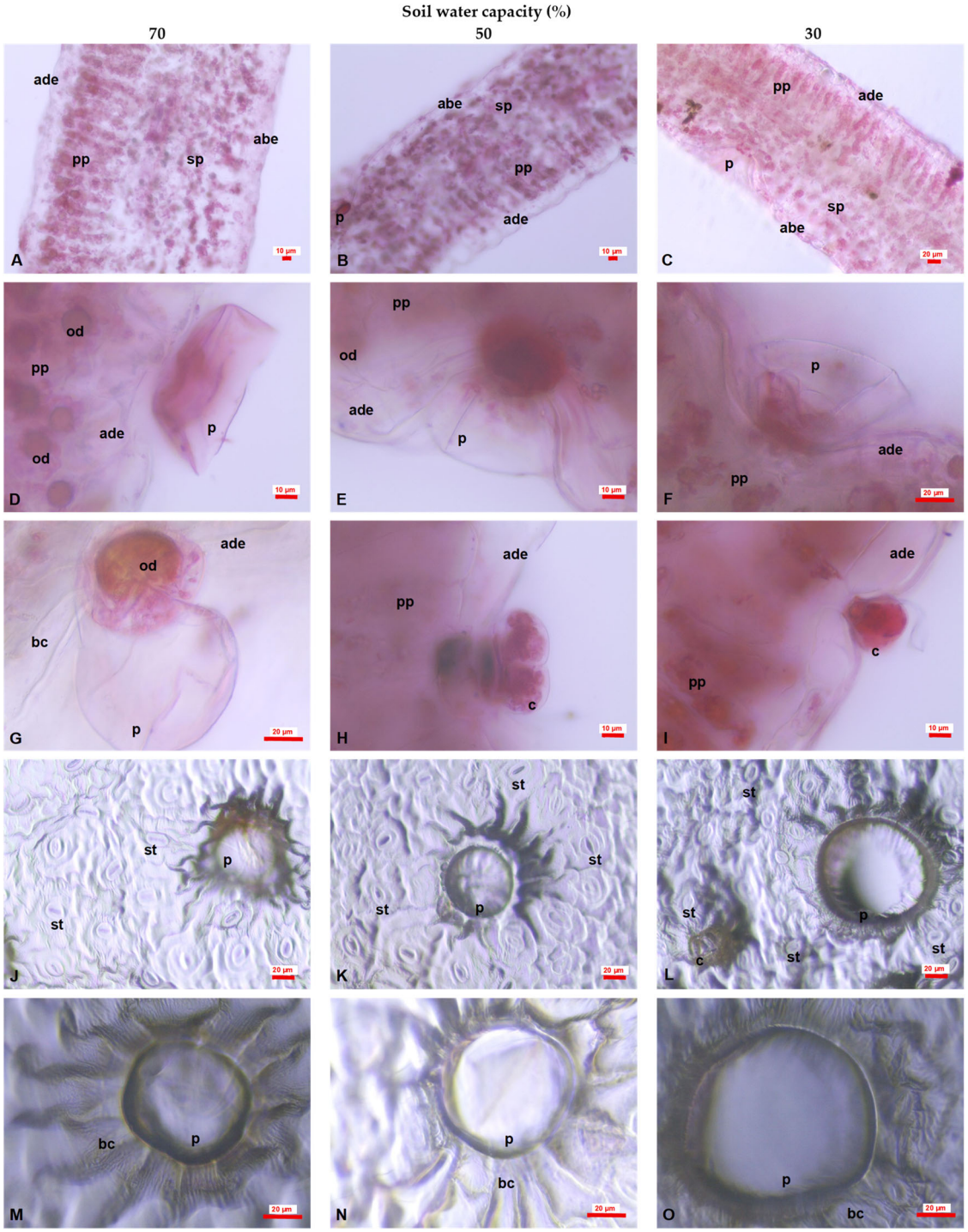

Figure 4. Effects of three soil water capacity levels (SWC70, SWC50, and SWC30) on leaf microanatomical characteristics of *Ocimum tenuiflorum* L. (**A**–**C**) Transverse sections of leaf laminae showing leaf mesophyll (10×); scale bars: 10, 20 µm. (**D**–**G**) Peltate glandular trichomes showing round multicellular secretory head and short unicellular stalk (40×); scale bars: 10, 20 µm. (**H**,**I**) Capitate glandular trichomes with bicellular head and unicellular stalk (40×); scale bars: 10 µm. (**J**–**L**) Peltate glandular trichomes on the abaxial epidermis (20×); scale bars: 20 µm. (**M**–**O**) Peltate glandular trichomes (40×); scale bars: 20 µm. abe: abaxial epidermis; ade: adaxial epidermis; bc: basal epidermal cells; c: capitate glandular trichomes; od: oil drops; p: peltate glandular trichomes; pp: palisade parenchyma; sp: spongy parenchyma; st: stomata.

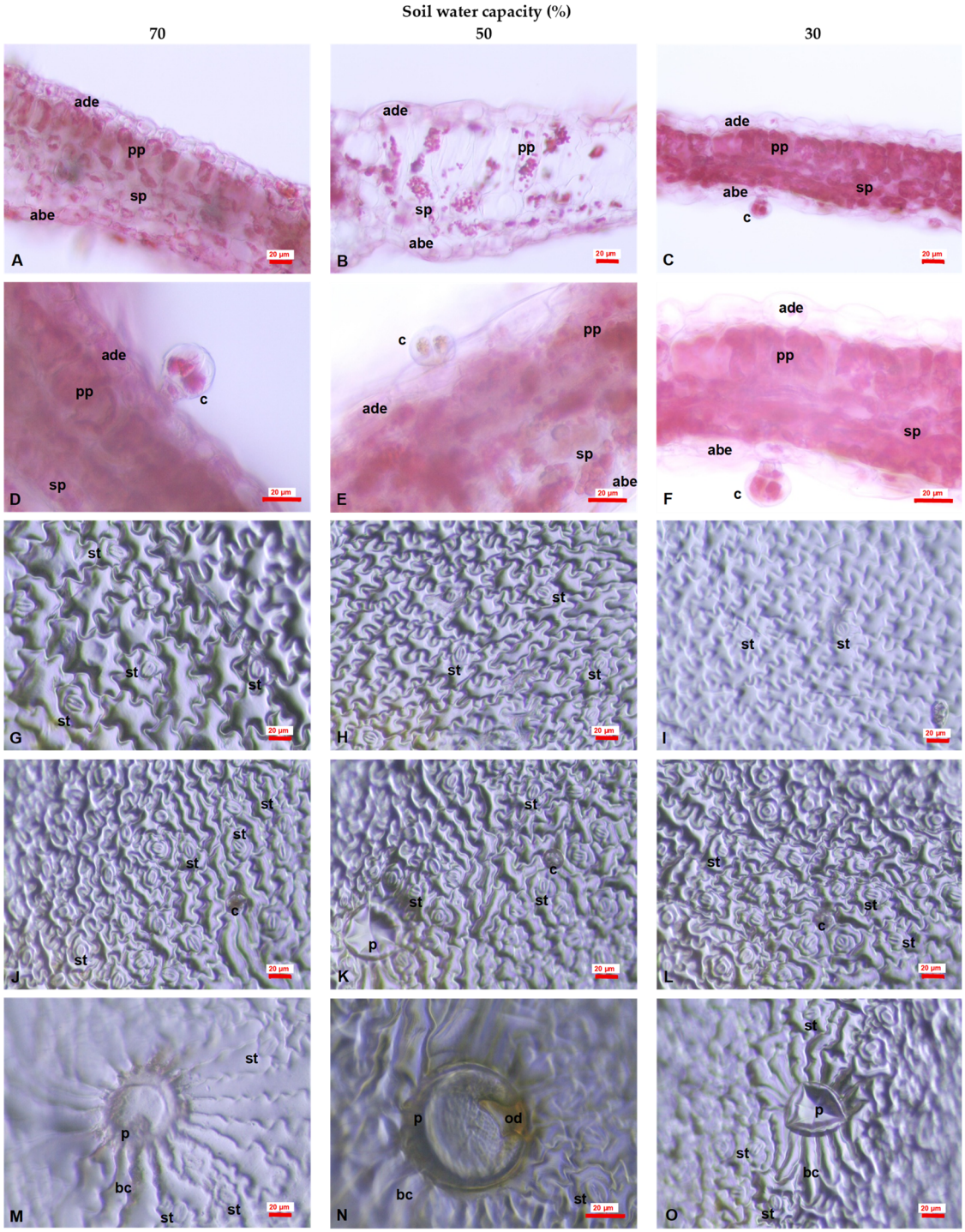

Figure 5. Effects of three soil water capacity levels (SWC70, SWC50, and SWC30) on leaf microanatomical characteristics of *Perilla frutescens* (L.) Britton. (**A**–**C**) Transverse sections of leaf laminae showing leaf mesophyll (20×); scale bars: 20 μm. (**D**–**F**) Capitate glandular trichomes with bicellular head and unicellular stalk (40×); scale bars: 20 μm. (**G**–**I**) Adaxial epidermis layer with low stomata density (20×); scale bars: 20 μm. (**J**–**L**) Abaxial epidermis layer with high stomata density (20×); scale bars: 20 μm. (**M**) Peltate glandular trichomes with multicellular secretory head (20×); scale bars: 20 μm. (**N**) Peltate glandular trichomes with multicellular secretory head (40×); scale bars: 20 μm. (**O**) Peltate glandular trichomes with multicellular secretory head (20×); scale bars: 20 μm. abe: abaxial epidermis; ade: adaxial epidermis; bc: basal epidermal cells; c: capitate glandular trichomes; od: oil drops; p: peltate glandular trichomes; pp: palisade parenchyma; sp: spongy parenchyma; st: stomata.

Adaxial peltate trichome density increased under moderate drought across most species. Under severe stress, responses diverged: in *N. cataria*, density returned to control levels, whereas in *O. tenuiflorum* and *L. angustifolia*, it continued to increase, with the latter showing an increase of over 200% compared to the control.

In *N. cataria*, the density of abaxial peltate glandular trichomes significantly increased under moderate stress (50% SWC), rising from 3.84 to 9.32 trichomes mm^{-2}. However, under severe drought stress (30% SWC), this density declined to values similar to the control. In the other species, no significant differences were observed in abaxial peltate trichome density across treatments. The diameter of peltate trichomes showed an opposite trend, decreasing under moderate stress, particularly on both leaf surfaces *N. cataria*, and increasing under severe drought (Figure 6).

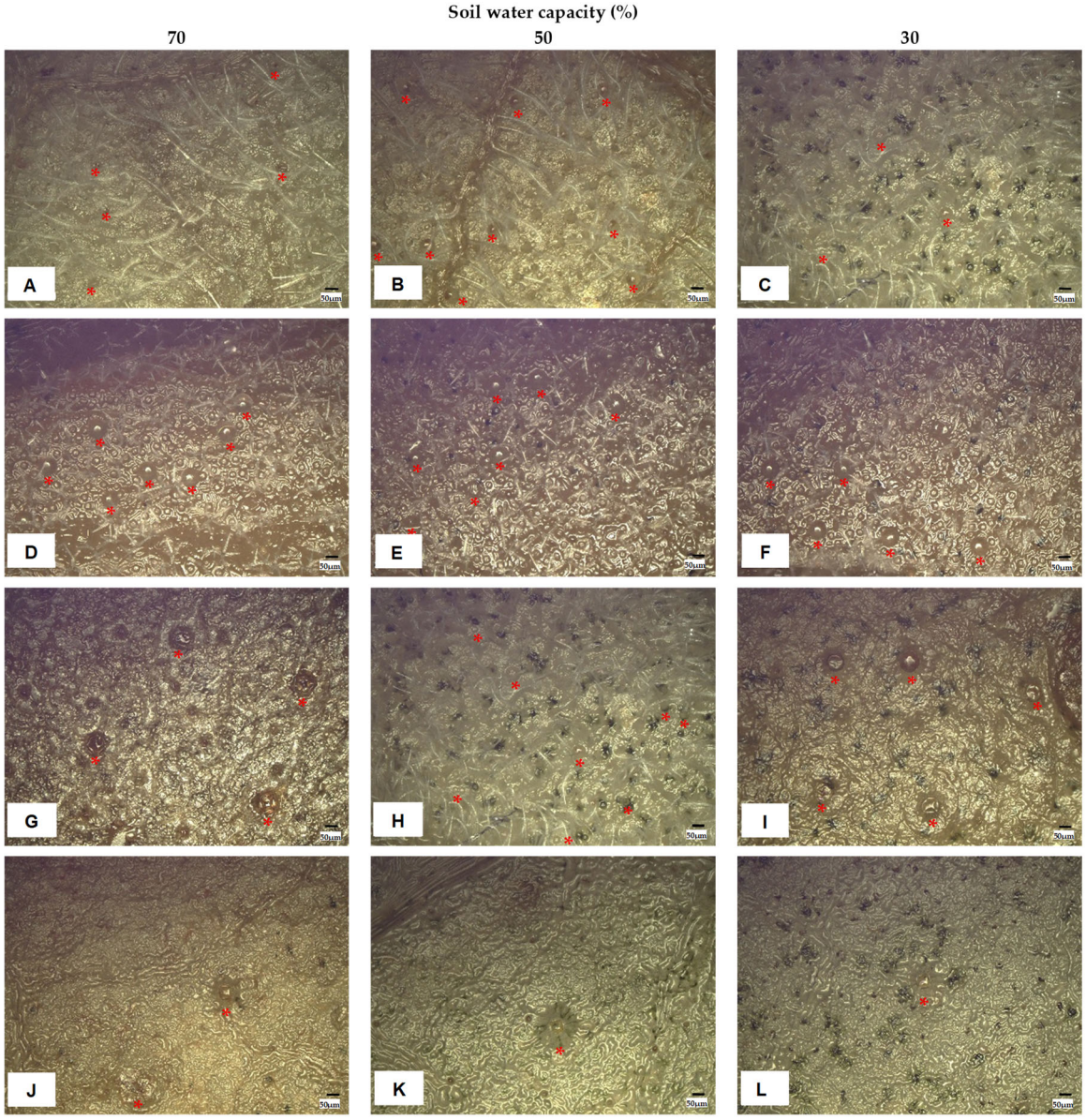

Figure 6. Effects of three soil water capacity levels (SWC70, SWC50, and SWC30) on the density of peltate glandular trichomes on the abaxial epidermis. (**A**–**C**) *Nepeta cataria* L. (**D**–**F**) *Lavandula angustifolia* Mill. (**G**–**I**) *Ocimum tenuiflorum* L. (**J**–**L**) *Perilla frutescens* (L.) Britton. Red asterisks indicate the peltate glandular trichomes. Images were captured using a Keyence VHX EA-300 digital microscope (Lens: ZS200, 200× magnification).

3.2.3. Stomatal Traits

Water deficit induced clear changes in stomatal morphology (Figure 7). Stomatal size generally decreased under drought, while stomatal density increased on both leaf surfaces.

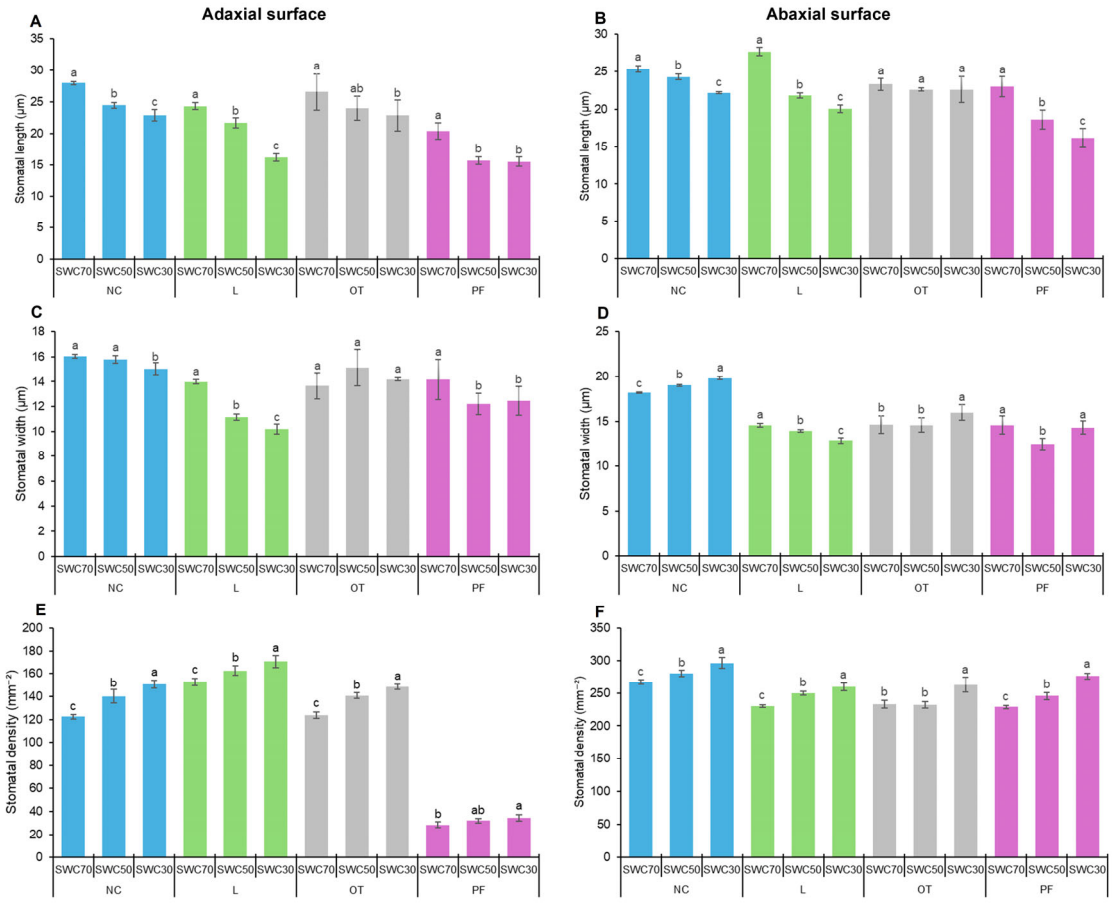

Figure 7. Effects of three soil water capacity levels SWC70 (control), SWC50 (moderate stress), and SWC30 (severe stress) on stomatal morphology and density across the adaxial and abaxial leaf surfaces. Bar charts represent stomatal length (**A**,**B**), stomatal width (**C**,**D**), and stomatal density (**E**,**F**) on the adaxial (left column) and abaxial (right column) surfaces. NC: *Nepeta cataria*; L: *Lavandula angustifolia*; OT: *Ocimum tenuiflorum*; PF: *Perilla frutescens*. Data represents the mean ± SD (n = 10). Different lowercase letters indicate significant differences between treatments within the same species according to Tukey's HSD post hoc test ($p < 0.05$).

A reduction in stomatal length was observed on both the adaxial and abaxial epidermises in all investigated species, with more pronounced decreases on the adaxial surface (Figure 7A,B). In *N. cataria*, moderate drought reduced adaxial stomatal length by 12.5%, with a smaller reduction on the abaxial surface (4.3%). Under severe drought, stomatal length decreased further on both surfaces.

A similar pattern was observed in *L. angustifolia*, where severe drought caused substantial reductions in stomatal length on both leaf surfaces (up to 33.4% adaxially). In *O. tenuiflorum*, reductions were more moderate, and no significant changes were detected on the abaxial surface (Figure 7B).

Stomatal width showed a more variable, species-dependent response (Figure 7C,D). *L. angustifolia* exhibited a clear reduction on both surfaces, whereas *N. cataria* showed an asymmetric pattern, with a slight decrease on the adaxial side and an increase on the abaxial surface under severe drought.

Stomatal density increased consistently with increasing drought intensity on both the adaxial (Figure 7E) and abaxial (Figure 7F) surfaces. This trend was most pronounced in *N. cataria* and *L. angustifolia*, where density increased significantly under both moderate and severe stress. In *O. tenuiflorum*, increases were more evident on the adaxial surface, while *P. frutescens* showed a more moderate response, with a significant increase observed only under severe drought.

3.3. Macro- and Microelement Concentrations

Drought stress significantly affected nutrient uptake and ion homeostasis in the investigated species. Tissue concentrations of several macro- and microelements were analyzed, and post hoc comparisons were performed for elements showing significant treatments effects and Species x Treatment interactions. The Tukey analysis (Table 2) focuses on Na, Ca, Mg, Ba, Li, S, Co, and Mn, revealing distinct, species-specific responses to water deficit.

Table 2. Concentrations of selected elements (mg kg^{-1} dry weight) in three Lamiaceae species (*Nepeta cataria* L., *Lavandula angustifolia* Mill., and *Ocimum tenuiflorum* L.) under three soil water capacity levels (SWC).

Element (mg/kg)	Treatment	*Nepeta cataria*	*Lavandula angustifolia*	*Ocimum tenuiflorum*
Co	SWC 70%	0.27 ± 0.05 a	0.32 ± 0.04 a	0.47 ± 0.43 a
	SWC 50%	0.26 ± 0.03 a	0.27 ± 0.09 a	0.32 ± 0.02 a
	SWC 30%	0.15 ± 0.04 b	0.29 ± 0.03 a	0.32 ± 0.02 a
Na	SWC 70%	104.6 ± 8.02 a	1284 ± 72.5 a	82.2 ± 30.1 a
	SWC 50%	74.6 ± 10.7 b	297.4 ± 9.5 b	73.9 ± 10.7 a
	SWC 30%	87 ± 6.7 ab	259.9 ± 8.8 b	68.5 ± 18.2 a
Ca	SWC 70%	17,770 ± 422 a	15,660 ± 937 a	20,416 ± 3709 a
	SWC 50%	14,250 ± 262 c	11,666 ± 148 b	17,046 ± 731 ab
	SWC 30%	16,203 ± 395 b	12,860 ± 409 b	14,370 ± 606 b
Mg	SWC 70%	4903 ± 325 a	5594 ± 142 a	5020 ± 597 a
	SWC 50%	4587 ± 253 a	5163 ± 942 a	4498 ± 668 a
	SWC 30%	4566 ± 247 a	4538 ± 179 a	4840 ± 54 a
Mn	SWC 70%	27.56 ± 0.9 c	20.83 ± 1.14 a	24.7 ± 10.13 a
	SWC 50%	67.1 ± 2 a	11.3 ± 0.62 b	16 ± 0.17 a
	SWC 30%	33.93 ± 2.1 b	12.97 ± 1.152 b	17.73 ± 1 a
Ba	SWC 70%	15.58 ± 0.68 a	35.04 ± 1.87 a	9.87 ± 4.22 a
	SWC 50%	7.43 ± 0.16 c	26.05 ± 0.58 b	7.29 ± 0.17 a
	SWC 30%	10.88 ± 0.6 b	27.16 ± 0.81 b	5.96 ± 0.03 a
Li	SWC 70%	0.15 ± 0.02 b	0.86 ± 0.05 a	0.45 ± 0.23 a
	SWC 50%	0.18 ± 0 a	0.43 ± 0.04 b	0.36 ± 0.02 a
	SWC 30%	0.17 ± 0.01 ab	0.56 ± 0.03 a	0.25 ± 0.01 a
S	SWC 70%	3058 ± 132 a	6647 ± 443 a	3368 ± 1247 a
	SWC 50%	3249 ± 67 a	4765 ± 303 b	2502 ± 76 a
	SWC 30%	3302 ± 203 a	4577 ± 60 b	2421 ± 171.47 a
B	SWC 70%	49.5 ± 2.55 a	37.63 ± 2.6 a	47.83 ± 18.89 a
	SWC 50%	30.73 ± 0.42 b	30.93 ± 2 b	32.66 ± 0.66 a
	SWC 30%	34.03 ± 2.61 b	29.56 ± 1.76 b	32.06 ± 1.05 a
Zn	SWC 70%	33.56 ± 1.98 a	67.03 ± 7.57 a	52.26 ± 20.58 a
	SWC 50%	28.03 ± 2.22 a	46.56 ± 1.28 b	38.43 ± 2.54 a
	SWC 30%	27.23 ± 6.21 a	41.73 ± 3.19 b	36.7 ± 2.25 a
Mo	SWC 70%	2.85 ± 0.09 a	5.8 ± 0.64 a	4.20 ± 1.67 a
	SWC 50%	1.73 ± 0.06 c	3.79 ± 0.14 b	2.92 ± 0.05 a
	SWC 30%	2.56 ± 0.02 b	3.59 ± 0.04 b	2.37 ± 0.09 a

Data are presented as means of three replicates ± SD. Statistical analyses were performed using ANOVA followed by Tukey's HSD post hoc test for elements where two-way ANOVA indicated a significant main effect or interaction. Means within a column followed by the same letter are not significantly different at $p < 0.05$.

Overall, the magnitude and direction of elemental changes varied among species. *Nepeta cataria* showed the most variable response, with pronounced fluctuations across treatments. For example, Mn concentration increased under moderate drought and declined under severe stress, although it remained above control levels. Several other elements (e.g., Ca, Ba, Mo, and B) showed a decrease under moderate stress followed by an increase under severe drought.

In contrast, *Ocimum tenuiflorum* maintained relatively stable elemental composition across treatments. Most elements showed no significant changes even under severe drought, with the exception of Ca, which decreased significantly at 30% SWC.

Lavandula angustifolia exhibited a consistent decline in the concentration of most elements under water deficit. Both moderate and severe drought reduced the levels of several elements (including Na, Ca, Mn, Ba, Li, S, B, Zn, and Mo), while Mg and Co remained relatively stable. Sodium showed the most pronounced decrease, reaching approximately one-quarter of the control level.

3.4. Correlations Among Micromorphological, Physiological, Phytochemical, and Elemental Traits

Pearson correlation analyses were performed separately for each species to examine relationships among physiological parameters, leaf micromorphology, elemental composition, and secondary metabolites. Results are presented as species-specific heatmaps (Figures S1–S3), while full correlation matrices are provided in the Supplementary Materials (Tables S1–S3).

Overall, correlation patterns differed markedly among species. Some relationships, particularly among elemental concentrations, were conserved, whereas associations between anatomical traits and secondary metabolism were more species-specific.

Across species, relative water content (RWC) showed strong associations with both growth and stomatal characteristics. In *Nepeta cataria*, RWC was positively related to biomass and negatively associated with stomatal density and size, indicating consistent links between water status and leaf structural traits. Similar relationships were observed in *Lavandula angustifolia* where RWC was negatively correlated with cuticle thickness and stomatal density, while showing positive associations with stomatal size.

Strong relationships between leaf structure and secondary metabolism were observed, although their direction varied among species. In *N. cataria*, essential oil (EO) content was positively associated with spongy parenchyma thickness, while total flavonoid content (TFC) showed an opposite pattern. In *L. angustifolia*, both EO and TFC were positively related to mesophyll and parenchyma thickness.

In *O. tenuiflorum*, flavonoid accumulation was strongly associated with multiple anatomical traits, including stomatal density and glandular trichome density, as well as trichome size. In contrast, EO content showed a negative relationship with mesophyll thickness.

The relationship between EO and TFC differed among species. In *N. cataria*, a strong negative association was observed between the two metabolites, whereas in *L. angustifolia*, EO and TFC were positively correlated.

Elemental concentrations were generally strong and consistent across species. In *N. cataria*, strong positive relationships were observed among Ca, Sr, and Ba, as well as between B and Ba. Similar patterns were detected in *O. tenuiflorum*, where several elements (e.g., Ba-Sr, K-Mn, and B with S, K, and P) showed very strong positive associations.

Despite some common trends, each species exhibited a distinct correlation network. *N. cataria* was characterized by strong interactions among water status, stomatal traits, and secondary metabolism. *L. angustifolia* showed a pronounced association between structural

traits and metabolite accumulation, whereas *O. tenuiflorum* displayed a network dominated by relationships between flavonoids and anatomical parameters.

4. Discussion

Global climate change is increasing the frequency and intensity of drought events, making water deficit one of the most critical abiotic stressors limiting plant productivity and secondary metabolism. However, drought does not simply suppress plant growth; it induces a complex cascade of adaptive responses operating across multiple levels of biological organizations, from gene expression to tissue structure [72]. The present results demonstrate that examined Lamiaceae species (*Nepeta cataria*, *Lavandula angustifolia*, *Ocimum tenuiflorum*, and *Perilla frutescens*) to not respond uniformly to water deficit, but instead exhibit distinct, species-specific strategies involving coordinated anatomical and biochemical adjustments [73]. A key initiating factor in these responses is the decline in plant water status, as reflected by reduced relative water content (RWC), which directly affects cellular turgor. Reduced turgor pressure limits cell expansion and triggers structural modifications of the leaf, including cuticle thickening and changes in stomatal and trichome density, all of which contribute to improved water retention under stress conditions. These anatomical adjustments are closely linked to changes in secondary metabolism. Modifications in glandular trichome density and structure influence the synthesis and storage capacity of essential oils, while shifts in cellular metabolism under stress promote the accumulation of protective compounds such as flavonoids. In parallel, reduced transpiration affects nutrient transport and rhizosphere interactions, leading to altered macro- and microelement uptake and a reorganization of ion homeostasis under drought conditions such as essential oils and flavonoids. In parallel, reduced transpiration alters the rhizosphere.

4.1. Micromorphological Reconfiguration as the Primary Driver of Drought Adaptation

The initial phase of drought adaptation involves structural reorganization of leaf tissues to limit water loss and maintain physiological functions [38,41]. Leaf anatomical traits play a central role in this process, as they directly influence water balance, gas exchange, and secondary metabolism. In the present study, the relationship between relative water content (RWC) and micromorphological traits highlights that the investigated species employ distinct structural strategies to cope with water deficit, consistent with previous findings in Lamiaceae species [74–76].

In *Nepeta cataria*, drought response is primarily associated with changes on stomatal density, representing a rapid and flexible drought-avoidance mechanisms. The negative relationship between RWC and stomatal density suggests that reduced water availability limits epidermal cell expansion during leaf development, resulting in smaller cells and higher stomatal density per unit area [77]. This structural adjustment likely enhances the capacity for rapid stomatal regulations, allowing more efficient control of transpiration under fluctuating water availability [78–80].

In contrast, *Lavandula angustifolia* exhibited pronounced modifications in epidermal and cuticular structures, indicating a strategy focused on minimizing non-stomatal water loss. The substantial increase in cuticle thickness under drought conditions reflects a well-documented xeromorphic adaptation that strengthens the barrier against cuticular transpiration [81,82]. In parallel, the observed reduction in stomatal dimensions under water deficit suggests a shift toward smaller, more responsive stomata, which are generally associated with improved control of gas exchange under stress conditions [83,84].

Ocimum tenuiflorum, a more mesophytic species, exhibited a different tissue-level strategy [85]. Lower RWC was associated with an apparent thickening of the upper epidermis and palisade parenchyma. Although seemingly counterintuitive, such thickening

is a well-documented feature of drought-induced xeromorphy [86]. Under optimal water supply, high turgor promotes cell elongation and leaf expansion, resulting in relatively thinner tissues. In contrast, water deficit restricts cell expansion, leading to smaller, more densely packed cells and a more compact structure [77,87]. This anatomical adjustment likely reduces specific leaf area and decreases the transpirational surface.

In *Perilla frutescens*, severe drought led to a contrasting response, characterized by a reduction in mesophyll and leaf thickness, indicating structural destabilization under stress. Similar patterns have been reported in drought-sensitive species, where rapid declines in water status lead to tissue shrinkage and impaired leaf integrity [76,88]. The concurrent increase in epidermal thickness, despite the absence of pronounced cuticular development, may represent a compensatory adjustment that contributes to partial protection of internal tissue.

Although this study was conducted under controlled conditions and included a limited number of species, the observed patterns suggest that drought adaptation in Lamiaceae involves multiple structural strategies, ranging from stomatal regulation to cuticular reinforcement and tissue compaction.

4.2. The Anatomical Basis of Secondary Metabolism: Trade-Offs and Compartmentalization

Beyond structural modifications, drought-induced water deficit alters internal biochemical processes, particularly the allocation of resources toward secondary metabolism [89]. Members of the Lamiaceae family are widely recognized for their high essential oil (EO) and total flavonoid content (TFC), both of which contribute to plant tolerance to biotic and abiotic stresses [90–92]. In agreement with previous studies [93–96], the present results indicate that the coordination between secondary metabolic biosynthesis and their histological localization follow distinct, species-specific adaptive strategies [97].

Due to severe structural degradation, *P. frutescens* exhibited limited metabolic activity, restricting detailed phytochemical evaluation. In contrast, *N. cataria*, *L. angustifolia*, and *O. tenuiflorum* provided sufficient data to explore the relationships between anatomical traits and phytochemical responses.

In *N. cataria*, drought stress was associated with reduced EO accumulation and increased TFC, consistent with previous findings [17,23,98,99]. The strong negative correlation between these metabolites suggests a trade-off in carbon allocation, where stress conditions favor flavonoid biosynthesis over terpenoid production. This shift is consistent with carbon partitioning theories [100,101], which propose that limited resources are redistributed between competing metabolic pathways. The association between spongy paranchyma thickness and metabolite levels further indicates that anatomical organization may influence this balance, with more developed internal tissue supporting terpenoid accumulation.

In *Lavandula angustifolia*, EO and TFC both peaked under moderate drought stress, in agreement with earlier studies [49,102–105]. Their coordinated increase is consistent with a hermetic response, in which moderate stress enhances secondary metabolite production without causing severe cellular damage. This pattern may reflect the activation of complementary defense mechanisms. In lavender, essential oils are thought to contribute to thermoregulation and herbivore deterrence, whereas flavonoids provide antioxidant protection [95,106–109]. The positive association between leaf lamina thickness and both EO and TFC further supports a link between anatomical development and metabolic capacity. In contrast, the negative relationship between mesophyll thickness and EO content suggests that metabolite accumulation may be more closely related to epidermal and cuticular tissues than to internal mesophyll structure.

O. tenuiflorum exhibits a distinct strategy characterized by strong spatial coordination between anatomical structures and metabolite accumulation. This pattern is consistent with the observations of Farouk and Omar [104], who reported drought-induced physiological and ultrastructural modifications associated with oxidative defense in sweet basil. While some studies reported reduced essential oil production under drought [110], our findings consistent with Mulugeta et al. [25] and Kalamartzis et al. [111] indicate increased EO and TFC under water deficit.

The strong association between flavonoid accumulation and palisade parenchyma suggests functional localization of these compounds in light-exposed tissues, where they act as UV filters and antioxidants [29,112]. In addition, the increased density of glandular trichomes under drought conditions likely contributes both to enhanced metabolite production and to physical protection through reduced transpiration and increased reflectance.

Overall, these results highlight that leaf anatomical organization plays a key role in regulating the balance between secondary metabolic pathways under drought stress. However, given that this study was conducted under controlled conditions, these relationships should be interpreted with caution when extrapolating to field environments.

4.3. Trichome Dynamics: The Intersection of Physical Shielding and Chemical Factories

The density and morphology of glandular trichomes (both peltate and capitate) represent a key anatomical link between physical drought adaptation and secondary metabolism in the Lamiaceae family. While trichome morphology shows considerable interspecific variability [113,114], these epidermal structures also show pronounced phenotypic plasticity in response to abiotic stressors [115]. In the present study, progressive water deficit generally resulted in an increase in glandular trichome density across the studied species, in agreement with previous reports. For example, Mulugeta et al. [24] observed a similar increase in glandular hair density under severe drought in other *Ocimum* species, a trend further supported by Li et al. [116].

An increased trichome density likely serves a dual function under drought conditions. Physically, a denser trichome layer can enhance boundary layer resistance, thereby reducing transpiration and reflecting excess solar radiation, which helps protect underlying tissues from photoinhibition and thermal stress. Chemically, peltate trichomes act as the primary sites of essential oil biosynthesis and storage [24], linking structural changes directly to secondary metabolite production. It should be noted that part of the observed increase in trichome density may result from a "concentration effect" caused by reduced leaf expansion under water deficit, leading to a higher number of trichomes per unit area. In addition, variation in trichome size appears to be associated with phytochemical responses. In *Ocimum tenuiflorum*, the strong association between TFC and both the density and diameter of peltate trichomes suggests that these structures actively contribute to the production of protective metabolites.

In contrast, the reduction in peltate trichome density observed on *Nepeta cataria* under severe drought coincided with decreased essential oil accumulation. This pattern may indicate that, under severe stress, the structural and metabolic capacity for terpene biosynthesis is limited, potentially resulting in a shift toward alternative defense strategies that require lower metabolic investment.

4.4. Ionomic Profiles: Geochemical Constraints and Luxury Consumption

Drought-induced anatomical and transpirational changes inevitably influence the root-to-shoot transport of mineral elements. The present results indicate that macro- and microelement uptake is governed by both general physicochemical principles and species-specific physiological regulation [27].

Across all investigated species, strong positive associations were observed among the alkaline earth metals (Ca, Sr, and Ba), reflecting their similar chemical properties. Due to limited selectivity in root cation transport systems, these elements are often taken up simultaneously, with Sr and Ba entering plant tissue via pathways similar to those of calcium, including apoplastic transport [117,118].

Species-specific differences were most pronounced for microelements. In *N. cataria*, an antagonistic relationship between manganese and molybdenum suggests competitive interactions in uptake or internal transport. In *L. angustifolia*, coordinated variation among sulfur, molybdenum, and zinc indicates a potential linkage between nutrient metabolism and detoxication processes [118,119].

The ionomic profile of *Ocimum tenuiflorum* was particularly notable, showing strong positive association among several elements (B, S, K, P, Mn, and Zn). This pattern is consistent with the phenomenon of "luxury consumption," commonly observed in fast-growing species, where elevated transpirational flux promotes nutrient uptake beyond immediate metabolic demand [100,120]. The close relationship between boron and potassium is especially relevant, as boron plays a role in membrane stability and may influence K-dependent transport processes and stomatal regulation.

Overall, these results indicate that drought responses in Lamiaceae species involve coordinated adjustments in ion uptake and distribution, closely linked to anatomical and physiological changes. However, given the controlled experimental conditions, these patterns should be interpreted cautiously when extrapolating to field environments.

4.5. Agronomic Implications

The observed micromorphological, phytochemical, and ionomic interactions indicate that water management in medicinal and aromatic plant cultivation should be species-specific rather than uniform. To optimize the production of target compounds, irrigation strategies must consider the distinct stress thresholds and anatomical constraints of each species. Moderate water deficit may function as an effective agronomic tool by inducing hormetic responses and enhancing essential oil production *in Lavandula angustifolia*. In contrast, severe drought in *Nepeta cataria* leads to reduced terpene biosynthesis due to anatomical limitations and carbon allocation trade-offs between metabolic pathways. Therefore, understanding species-specific structural–metabolic relationships is essential for optimizing both yield and quality of secondary metabolites under increasingly variable climatic conditions [24,25,33].

These findings suggest that maintaining approximately 50% soil water capacity may represent an optimal compromise between plant growth and secondary metabolite production in several Lamiaceae species. These findings emphasize the importance of species-specific irrigation strategies and highlight the potential of controlled deficit irrigation as a tool to optimize both plant resilience and the accumulation of high-value bioactive compounds.

5. Conclusions

This study indicates that drought adaptation in the Lamiaceae family is not a uniform physiological process but rather a highly species-specific cascade of micromorphological, ionomic, and biochemical adjustments. By integrating leaf microanatomy with secondary metabolite profiling, our results revealed that leaf structural traits strongly influence metabolic responses under water deficit.

Three distinct adaptive response strategies were identified. (i) *Lavandula angustifolia* Mill. exhibits a structural, synergist strategy, relying on substantial cuticular thickening and reduced stomatal size to limit water loss. It displays a hormetic response to moderate

drought, with a simultaneous increase in essential oil (EO) and total flavonoid content (TFC), forming a dual chemical defense system. (ii) *Nepeta cataria* L. follows a dynamic avoidance strategy, utilizing rapid adjustments in stomatal density to regulate transpiration. Under severe stress, it exhibits a pronounced carbon-allocation trade-off, reducing terpene (EO) production in favor of flavonoid synthesis to maintain cellular protection. (iii) *Ocimum tenuiflorum* L. employs a xeromorphic compartmentalization strategy, characterized by tissue compaction and relatively stable ionomic homeostasis. In this species, flavonoid accumulation appears to be associated with the dense upper palisade parenchyma, contributing to enhanced photoprotection. In contrast, *Perilla frutescens* displays a stress-sensitive structural response, characterized by reduced mesophyll thickness and stomatal size, combined with increased stomatal and capitate glandular trichome densities. Together with the thickening of the adaxial epidermis, these changes reflect xeromorphic acclimation aimed at minimizing transpirational water loss and protecting internal tissues.

Although this study examined only four species, the identified response patterns likely represent broader adaptive strategies within the Lamiaceae family.

From an agronomic perspective, these results indicate that precision agriculture and irrigation management in Lamiaceae species cultivation cannot rely on generalized protocols. To optimize the yield and quality of bioactive compounds, cultivation practices must be tailored to the specific stress thresholds of each species. For instance, moderate irrigation may enhance EO production in *Lavandula angustifolia*, whereas similar conditions may suppress terpene biosynthesis in *Nepeta cataria* due to metabolic trade-offs.

Future research should focus on the molecular and transcriptomic mechanisms regulating these micromorphological-metabolic interactions. Understanding these processes will be essential for breeding climate-resilient cultivars capable of maintaining high secondary metabolite production under increasingly arid global climate.

Supplementary Materials: The following supporting information can be downloaded at: https://www.mdpi.com/article/10.3390/horticulturae12040470/s1, Figure S1: Pearson correlation matrix of *Nepeta cataria* L.; Figure S2: Pearson correlation matrix of *Lavandula angistofolia* Mill.; Figure S3: Pearson correlation matrix heatmaps of *Ocimum tenuiflorum* L.; Table S1: Pearson correlation matrix heatmaps of *Nepeta cataria* L.; Table S2: Pearson correlation matrix heatmaps *Lavandula angustifolia* Mill.; Table S3: Pearson correlation matrix of *Ocimum tenuiflorum* L.

Author Contributions: Conceptualization, C.T. and B.T.; methodology, C.T., B.T., E.B. and S.V.; formal analysis, C.T., E.B. and B.T.; investigation, C.T., E.B. and S.V.; data curation, C.T., E.B. and S.V.; writing—original draft preparation, C.T. and B.T.; writing—review and editing, C.T. and B.T.; visualization, C.T.; supervision, C.T. and B.T.; project administration, C.T. and B.T.; funding acquisition, B.T. All authors have read and agreed to the published version of the manuscript.

Funding: This research received no external funding.

Data Availability Statement: The original contributions presented in this study are included in the article and Supplementary Materials. Further inquiries can be directed to the corresponding author.

Acknowledgments: The authors thank Rebeka Szegedi for their assistance in seedling cultivation, planting, plant care, and measurement.

Conflicts of Interest: The authors declare no conflicts of interest.

References

1. Zhao, F.; Chen, Y.P.; Salmaki, Y.; Drew, B.T.; Wilson, T.C.; Scheen, A.C.; Celep, F.; Bräuchler, C.; Bendiksby, M.; Wang, Q.; et al. An updated tribal classification of Lamiaceae based on plastome phylogenomics. *BMC Biol.* **2021**, *19*, 2. [CrossRef] [PubMed] [PubMed Central]
2. Harley, R.M.; Atkins, S.; Budantsev, A.L.; Cantino, P.D.; Conn, B.J.; Grayer, R.; Harley, M.M.; de Kok, R.; Krestovskaja, T.; Morales, R.; et al. Labiatae. In *Flowering Plants—Dicotyledons. The Families and Genera of Vascular Plants*; Kadereit, J.W., Ed.; Springer: Berlin/Heidelberg, Germany, 2004; Volume 7. [CrossRef]
3. Almatroodi, S.A.; Alsahli, M.A.; Almatroudi, A.; Rahmani, A.H. *Ocimum sanctum*: Role in Diseases Management Through Modulating Various Biological Activity. *Pharmacogn. J.* **2020**, *12*, 1198–1205. [CrossRef]
4. Carović-Stanko, K.; Petek, M.; Grdiša, M.; Pintar, J.; Bedeković, D.; Herak Ćustić, M.; Satovic, Z. Medicinal plants of the family Lamiaceae as functional foods—A review. *Czech J. Food Sci.* **2016**, *34*, 377–390. [CrossRef]
5. Chaudhary, A.; Sharma, S.; Mittal, A.; Gupta, S.; Dua, A. Phytochemical and antioxidant profiling of *Ocimum sanctum*. *J. Food Sci. Technol.* **2020**, *57*, 3852–3863. [CrossRef] [PubMed] [PubMed Central]
6. Avasiloaiei, D.I.; Calara, M.; Brezeanu, P.M.; Murariu, O.C.; Brezeanu, C. On the Future Perspectives of Some Medicinal Plants within Lamiaceae Botanic Family Regarding Their Comprehensive Properties and Resistance Against Biotic and Abiotic Stresses. *Genes* **2023**, *14*, 955. [CrossRef]
7. Sun, J.; Sun, P.; Kang, C.; Zhang, L.; Guo, L.; Kou, Y. Chemical composition and biological activities of essential oils from six Lamiaceae folk medicinal plants. *Front. Plant Sci.* **2022**, *13*, 919294. [CrossRef]
8. Nieto, G. Biological activities of three essential oils of the Lamiaceae family. *Medicines* **2017**, *4*, 63. [CrossRef]
9. Giuliani, C.; Giovanetti, M.; Lupi, D.; Mesiano, M.P.; Barilli, R.; Ascrizzi, R.; Flamini, G.; Fico, G. Tools to Tie: Flower Characteristics, VOC Emission Profile, and Glandular Trichomes of Two Mexican Salvia Species to Attract Bees. *Plants* **2020**, *9*, 1645. [CrossRef]
10. Fahn, A. Structure and function of secretory cells. In *Advances in Botanical Research. Incorporating Advances in Plant Pathology. Plant Trichomes*; Hallahon, D.L., Gray, J.C., Eds.; Academic Press: London, UK, 2000; Volume 31, pp. 37–75.
11. Werker, E.; Ravid, U.; Putievsky, E. Structure of glandular hairs and identification of the main components of their secreted material in some species of the Labiatae. *Isr. J. Plant Sci.* **1985**, *34*, 31–45. [CrossRef]
12. Werker, E. Function of essential oil-secreting glandular hairs in aromatic plants of the Lamiaceae. *Flavour Fragr. J.* **1993**, *8*, 249–255. [CrossRef]
13. Huang, S.S.; Kirchoff, B.K.; Liao, J.P. The capitate and peltate glandular trichomes of *Lavandula pinnata* L. (Lamiaceae): Histochemistry, ultrastructure, and secretion. *J. Torrey Bot. Soc.* **2008**, *135*, 155–167. [CrossRef]
14. McCaskill, D.; Croteau, R. Monoterpene and sesquiterpene biosynthesis in glandular trichomes of peppermint (*Mentha* × *piperita*) rely exclusively on plastid-derived isopentenyl diphosphate. *Planta* **1995**, *197*, 49–56. [CrossRef]
15. Baran, P.; Aktaş, K.; Özdemir, C. Structural investigation of the glandular trichomes of endemic *Salvia smyrnea* L. *S. Afr. J. Bot.* **2010**, *76*, 572–578. [CrossRef]
16. Kahraman, A.; Celep, F.; Dogan, M. Anatomy, trichome morphology and palynology of *Salvia chrysophylla* Stapf (Lamiaceae). *S. Afr. J. Bot.* **2010**, *76*, 187–195. [CrossRef]
17. Lungoci, C.; Motrescu, I.; Filipov, F.; Jitareanu, C.D.; Teliban, G.-C.; Ghitau, C.S.; Puiu, I.; Robu, T. The Impact of Salinity Stress on Antioxidant Response and Bioactive Compounds of *Nepeta cataria* L. *Agronomy* **2022**, *12*, 562. [CrossRef]
18. Karray-Bouraoui, N.; Rabhi, M.; Neffati, M.; Baldan, B.; Ranieri, A.; Marzouk, B.; Lachaâl, M.; Smaoui, A. Salt effect on yield and composition of shoot essential oil and trichome morphology and density on leaves of *Mentha pulegium*. *Ind. Crops Prod.* **2009**, *30*, 338–343. [CrossRef]
19. Kowalski, R.; Kowalska, G.; Jankowska, M.; Nawrocka, A.; Kałwa, K.; Pankiewicz, U.; Włodarczyk-Stasiak, M. Secretory Structures and Essential Oil Composition of Selected Industrial Species of Lamiaceae. *Acta Sci. Pol. Hortorum Cultus* **2019**, *18*, 53–69. [CrossRef]
20. Soliman, S.S.M.; Abouleish, M.; Abou-Hashem, M.M.M.; Hamoda, A.M.; El-Keblawy, A.A. Lipophilic Metabolites and Anatomical Acclimatization of *Cleome amblyocarpa* in the Drought and Extra-Water Areas of the Arid Desert of UAE. *Plants* **2019**, *8*, 132. [CrossRef]
21. Zhou, Y.; Tang, N.; Huang, L.; Zhao, Y.; Tang, X.; Wang, K. Effects of Salt Stress on Plant Growth, Antioxidant Capacity, Glandular Trichome Density, and Volatile Exudates of *Schizonepeta tenuifolia* Briq. *Int. J. Mol. Sci.* **2018**, *19*, 252. [CrossRef]
22. Muravnik, L.E. The Structural Peculiarities of the Leaf Glandular Trichomes: A Review. In *Plant Cell and Tissue Differentiation and Secondary Metabolites*; Ramawat, K., Ekiert, H., Goyal, S., Eds.; Reference Series in Phytochemistry; Springer: Cham, Switzerland, 2020. [CrossRef]
23. Aćimović, M.; Lončar, B.; Rat, M.; Cvetković, M.; Stanković Jeremić, J.; Pezo, M.; Pezo, L. Seasonal Variation in Volatile Profiles of Lemon Catnip (*Nepeta cataria* var. *citriodora*) Essential Oil and Hydrolate. *Horticulturae* **2025**, *11*, 862. [CrossRef]
24. Mulugeta, S.M.; Radácsi, P. Influence of drought stress on growth and essential oil yield of *Ocimum* species. *Horticulturae* **2022**, *8*, 175. [CrossRef]

25. Mulugeta, S.M.; Hunegnaw, A.T.; Hári, K.; Radácsi, P. Biomass Production and Volatile Oil Accumulation of *Ocimum* Species Subjected to Drought Stress. *Horticulturae* **2025**, *11*, 1266. [CrossRef]
26. Simon, J.E.; Reiss-Bubenheim, D.; Joly, R.J.; Charles, D.J. Water stress-induced alterations in essential oil content and composition of sweet basil. *J. Essent. Oil Res.* **1992**, *4*, 71–75. [CrossRef]
27. García-Caparrós, P.; Romero, M.J.; Llanderal, A.; Cermeño, P.; Lao, M.T.; Segura, M.L. Effects of Drought Stress on Biomass, Essential Oil Content, Nutritional Parameters, and Costs of Production in Six *Lamiaceae* Species. *Water* **2019**, *11*, 573. [CrossRef]
28. Bidgoli, R.D. Effect of drought stress on some morphological characteristics, quantity and quality of essential oil in Rosemary (*Rosmarinus officinalis* L.). *Adv. Med. Plant Res.* **2018**, *6*, 40–45. [CrossRef]
29. Al-Huqail, A.; El-Dakak, R.M.; Sanad, M.N.; Badr, R.H.; Ibrahim, M.M.; Soliman, D.; Khan, F. Effects of climate temperature and water stress on plant growth and accumulation of antioxidant compounds in sweet basil (*Ocimum basilicum* L.) leafy vegetable. *Scientifica* **2020**, *2020*, 3808909. [CrossRef]
30. Usano-Alemany, J.; Palá-Paúl, J.; Herráiz-Peñalver, D. Temperature stress causes different profiles of volatile compounds in two chemotypes of *Salvia lavandulifolia*. *Vahl. Biochem. Syst. Ecol.* **2014**, *54*, 166–171. [CrossRef]
31. Panche, A.N.; Diwan, A.D.; Chandra, S.R. Flavonoids: An overview. *J. Nutr. Sci.* **2016**, *5*, e47. [CrossRef]
32. Anjum, S.A.; Xie, X.; Wang, L.C.; Saleem, M.F.; Man, C.; Lei, W. Morphological, physiological and biochemical responses of plants to drought stress. *Afr. J. Agric. Res.* **2011**, *6*, 2026–2032.
33. Mulugeta, S.M.; Sárosi, S.; Radácsi, P. Physio-morphological trait and bioactive constituents of *Ocimum* species under drought stress. *Ind. Crops Prod.* **2023**, *205*, 117545. [CrossRef]
34. Amiri, H.; Dousty, B.; Hosseinzedeh, S.R. Water stress-induced changes of morphological, physiological and essential oil compounds in *Thymus eriocalyx* from Iran. *J. Essent. Oil Bear. Plants* **2018**, *21*, 1210–1223. [CrossRef]
35. Tan, U.; Gören, H.K. Comprehensive evaluation of drought stress on medicinal plants: A meta-analysis. *PeerJ.* **2024**, *12*, e17801. [CrossRef] [PubMed] [PubMed Central]
36. Lianopoulou, V.; Bosabalidis, A.M.; Patakas, A.; Panteris, D.L.E. Effects of chilling stress on leaf morphology, anatomy, ultrastructure, gas exchange, and essential oils in the seasonally dimorphic plant *Teucrium polium* (Lamiaceae). *Acta Physiol. Plant.* **2014**, *36*, 2271–2281. [CrossRef]
37. Sanders, G.J.; Arndt, S.K. Osmotic Adjustment Under Drought Conditions. In *Plant Responses to Drought Stress*; Aroca, R., Ed.; Springer: Berlin/Heidelberg, Germany, 2012. [CrossRef]
38. Yavas, I.; Jamal, M.A.; Din, K.U.; Ali, S.; Hussain, S.; Farooq, M. Drought-Induced Changes in Leaf Morphology and Anatomy: Overview, Implications and Perspectives. *Pol. J. Environ. Stud.* **2024**, *33*, 1517–1530. [CrossRef]
39. Driesen, E.; Van den Ende, W.; De Proft, M.; Saeys, W. Influence of Environmental Factors Light, CO_2, Temperature, and Relative Humidity on Stomatal Opening and Development: A Review. *Agronomy* **2020**, *10*, 1975. [CrossRef]
40. Driesen, E.; De Proft, M.; Saeys, W. Drought stress triggers alterations of adaxial and abaxial stomatal development in basil leaves increasing water-use efficiency. *Hortic. Res.* **2023**, *10*, uhad075. [CrossRef]
41. Bano, C.; Amist, N.; Singh, N.B. Morphological and anatomical modifications of plants for environmental stresses. In *Molecular Plant Abiotic Stress*; Roychoudhury, A., Tripathi, D., Eds.; John Wiley & Sons, Ltd.: Hoboken, NJ, USA, 2019; pp. 29–44. [CrossRef]
42. Seleiman, M.F.; Al-Suhaibani, N.; Ali, N.; Akmal, M.; Alotaibi, M.; Refay, Y.; Dindaroglu, T.; Abdul-Wajid, H.H.; Battaglia, M.L. Drought Stress Impacts on Plants and Different Approaches to Alleviate Its Adverse Effects. *Plants* **2021**, *10*, 259. [CrossRef]
43. Askary, M.; Behdani, M.A.; Parsa, S.; Mahmoodi, S.; Jamialahmadi, M. Water stress and manure application affect the quantity and quality of essential oil of *Thymus daenensis* and *Thymus vulgaris*. *Ind. Crops Prod.* **2018**, *111*, 336–344. [CrossRef]
44. Bistgani, Z.E.; Barker, A.V.; Hashemi, M. Physiology of medicinal and aromatic plants under drought stress. *Crop J.* **2024**, *12*, 330–339. [CrossRef]
45. Bistgani, Z.E.; Ataollah Siadat, S.; Bakhshandeh, A.; Pirbalouti, A.G.; Hashemi, M. Interactive effects of drought stress and chitosan application on physiological characteristics and essential oil yield of (*Thymus daenensis* Celak). *Crop J.* **2017**, *5*, 407–415. [CrossRef]
46. Vosoughi, N.; Gomarian, M.; Ghasemi Pirbalouti, A.; Khaghani, S.; Malekpoor, F. Essential oil composition and total phenolic, flavonoid contents, and antioxidant activity of sage (*Salvia officinalis* L.) extract under chitosan application and irrigation frequencies. *Ind. Crops Prod.* **2018**, *117*, 366–374. [CrossRef]
47. Bistgani, Z.E.; Siadat, A.S.; Bakhshandeh, A.; Ghasemi Pirbalouti, A.; Hashemi, M. Morpho-physiological and phytochemical traits of (*Thymus daenensis* Celak.) in response to deficit irrigation and chitosan application. *Acta Physiol. Plant.* **2017**, *39*, 231. [CrossRef]
48. Morshedloo, M.R.; Craker, L.E.; Salami, A.; Nazeri, V.; Sang, H.; Magg, F. Effect of prolonged water stress on essential oil content, compositions and gene expression patterns of mono- and sesquiterpene synthesis in two oregano (*Origanum vulgare* L.) subspecies. *Plant Physiol. Biochem.* **2017**, *111*, 119–128. [CrossRef] [PubMed]
49. Hosseini, R.; Heidari, M. Impact of drought stress on biochemical and molecular responses in lavender (*Lavandula angustifolia* Mill.): Effects on essential oil composition and antibacterial activity. *Front. Plant Sci.* **2025**, *16*, 1506660. [CrossRef]

50. Giuliani, C.; Bottoni, M.; Ascrizzi, R.; Milani, F.; Spada, A.; Papini, A.; Flamini, G.; Fico, G. Insight into micromorphology and phytochemistry of *Lavandula angustifolia* Mill. from Italy. *S. Afr. J. Bot.* **2023**, *153*, 83–93. [CrossRef]
51. Cho, J.; Park, H.; Heo, T.H.; Heo, T.H.; Sa, K.; Lee, J.K. Phylogenetic analysis of Perilla crop (*Perilla frutescens* L.) based on morphological characteristics and volatile substances. *Genet. Resour. Crop Evol.* **2025**, *72*, 2959–2976. [CrossRef]
52. Jiang, Z.; Zhou, P.; Shao, Y.; Zhang, Q.; Yue, W.; Qu, C.; Wu, Q. Applying quantitative spatial phenotypes analysis to the investigation of peltate glandular trichomes development pattern in *Perilla frutescens*. *Plant Methods* **2023**, *19*, 88. [CrossRef] [PubMed] [PubMed Central]
53. Radácsi, P.; Inotai, K.; Sárosi, S.; Hári, K.; Seidler-Łozykowska, K.; Musie, S.; Zámboriné, É.N. Effect of irrigation on the production and volatile compounds of Sweet basil cultivars (*Ocimum basilicum* L.). *Herba Pol.* **2020**, *66*, 14–24. [CrossRef]
54. Vukić, M.D.; Vuković, N.L.; Mladenović, M.; Tomašević, N.; Matić, S.; Stanić, S.; Sapienza, F.; Ragno, R.; Božović, M.; Kačániová, M. Chemical Composition of Various *Nepeta cataria* Plant Organs' Methanol Extracts Associated with In Vivo Hepatoprotective and Antigenotoxic Features as well as Molecular Modeling Investigations. *Plants* **2022**, *11*, 2114. [CrossRef]
55. Sharma, A.; Cooper, R.; Bhardwaj, G.; Cannoo, D.S. The genus Nepeta: Traditional uses, phytochemicals and pharmacological properties. *J. Ethnopharmacol.* **2021**, *268*, 113679. [CrossRef] [PubMed]
56. *MSZ 08-0206/2:1978*; Determination of the pH of Soil. Hungarian Standard Association: Budapest, Hungary, 1978. (In Hungarian)
57. *MSZ 08-0210:1977*; Testing Organic Carbon Content in Soils. Hungarian Standard Association: Budapest, Hungary, 1977. (In Hungarian)
58. *MSZ 08-0458:1980*; Determination of Total Nitrogen Content in Soils. Hungarian Standard Association: Budapest, Hungary, 1980. (In Hungarian)
59. *MSZ 20135:1999*; Determination of the Soluble Nutrient Element Content of the Soil. Hungarian Standard Association: Budapest, Hungary, 1999. (In Hungarian)
60. Reynolds, S.G. The gravimetric method of soil moisture determination Part I: A study of equipment, and methodological problems. *J. Hydrol.* **1970**, *11*, 258–273. [CrossRef]
61. Barykina, R.P. *Guide on Botanical Microtechique; Base and Methods*; MSU: Moscow, Russia, 2004; p. 312.
62. Hilu, K.W.; Randall, J.L. Convenient method for studying grass leaf epidermis. *Taxon* **1984**, *33*, 413–415. [CrossRef]
63. Gardner, S.D.L.; Taylor, G.; Bosac, C. Leaf growth of hybrid poplar following exposure to elevated CO_2. *N. Phytol.* **1995**, *131*, 81–90. [CrossRef]
64. Elagöz, V.; Han, S.S.; Manning, W.J. Acquired changes in stomatal characteristics in response to ozone during plant growth and leaf development of bush beans (*Phaseolus vulgaris* L.) indicate phenotypic plasticity. *Environ. Pollut.* **2006**, *140*, 395–405. [CrossRef]
65. García-Gutiérrez, E.; Ortega-Escalona, F.; Angeles, G. A novel, rapid technique for clearing leaf tissues. *Appl. Plant Sci.* **2020**, *8*, e11391. [CrossRef]
66. Mulugeta, S.M.; Pluhár, Z.; Radácsi, P. Phenotypic Variations and Bioactive Constituents among Selected *Ocimum* Species. *Plants* **2024**, *13*, 64. [CrossRef] [PubMed]
67. Sass, J.E. *Botanical Microtechnique*, 2nd ed.; Iowa State College Press: Ames, IA, USA, 1951.
68. Barrs, H.D. Determination of water deficits in plant tissues. In *Water Deficits and Plant Growth*; Koslowski, T.T., Ed.; Academic Press: New York, NY, USA, 1968; pp. 235–368.
69. Weatherley, P.E. Studies in the water relations of the cotton plant. I. The field measurement of water deficits in leaves. *N. Phytol.* **1950**, *49*, 81–97. [CrossRef]
70. Kim, D.O.; Chun, O.K.; Kim, Y.J.; Moon, H.Y.; Lee, C.Y. Quantification of polyphenolics and their antioxidant capacity in fresh plums. *J. Agric. Food Chem.* **2003**, *51*, 6509–6515. [CrossRef]
71. Hungarica, P. *Pharmacopoeia Hungarica*, 7th ed.; ResearchGate: Budapest, Hungary, 1986; pp. 395–398.
72. Gupta, A.; Rico-Medina, A.; Caño-Delgado, A.I. The physiology of plant responses to drought. *Science* **2020**, *368*, 266–269. [CrossRef] [PubMed]
73. Kulak, M. Recurrent drought stress effects on essential oil profile of Lamiaceae plants: An approach regarding stress memory. *Ind. Crops Prod.* **2020**, *154*, 112695. [CrossRef]
74. Bahreininejad, B.; Razmjoo, J.; Mirza, M. Influence of water stress on morpho-physiological and phytochemical traits in *Thymus daenensis*. *Int. J. Plant Prod.* **2013**, *7*, 155–166.
75. Govahi, M.; Ghalavand, A.; Nadjafi, F.; Sorooshzadeh, A. Comparing different soil fertility systems in Sage (*Salvia officinalis*) under water deficiency. *Ind. Crops Prod.* **2015**, *74*, 20–27. [CrossRef]
76. Wang, J.Y.; Xu, W.N.; Su, Y.; Zhang, B. Changes in Leaf Morphology and Anatomical Structure of Seedlings of Alfalfa and *Medicago falcata* L. under Drought Stress. *Acta Agric. Boreali-Sin.* **2023**, *38*, 228–236.
77. Tardieu, F.; Reymond, M.; Hamard, P.; Granier, C.; Muller, B. Spatial distributions of expansion rate, cell division rate and cell size in maize leaves: A synthesis of the effects of soil water status, evaporative demand and temperature. *J. Exp. Bot.* **2000**, *51*, 1505–1514. [CrossRef] [PubMed]

78. Franks, P.J.; Beerling, D.J. Maximum leaf conductance driven by CO_2 effects on stomatal size and density over geologic time. *Proc. Natl. Acad. Sci. USA* **2009**, *106*, 10343–10347. [CrossRef]
79. Petrík, P.; Petek-Petrík, A.; Lamarque, L.J.; Link, R.M.; Waite, P.; Ruehr, N.K.; Schuldt, B.; Maire, V. Linking stomatal size and density to water use efficiency and leaf carbon isotope ratio in juvenile and mature trees. *Physiol. Plant.* **2024**, *176*, e14619. [CrossRef]
80. Alongi, F.; Petek-Petrik, A.; Mukarram, M.; Torun, H.; Schuldt, B.; Petrík, P. Somatic drought stress memory affects leaf morpho-physiological traits of plants via epigenetic mechanisms and phytohormonal signaling. *Plant Gene* **2025**, *42*, 2352–4073. [CrossRef]
81. Riederer, M.; Schreiber, L. Protecting against water loss: Analysis of the barrier properties of plant cuticles. *J. Exp. Bot.* **2001**, *52*, 2023–2032. [CrossRef] [PubMed]
82. Sintaha, M.; Man, C.-K.; Yung, W.-S.; Duan, S.; Li, M.-W.; Lam, H.-M. Drought Stress Priming Improved the Drought Tolerance of Soybean. *Plants* **2022**, *11*, 2954. [CrossRef] [PubMed]
83. Blum, A. Osmotic adjustment is a prime drought stress adaptive engine in support of plant production. *Plant Cell Environ.* **2017**, *40*, 4–10. [CrossRef] [PubMed]
84. Szekely-Varga, Z.; González-Orenga, S.; Cantor, M.; Jucan, D.; Boscaiu, M.; Vicente, O. Effects of Drought and Salinity on Two Commercial Varieties of *Lavandula angustifolia* Mill. *Plants* **2020**, *9*, 637. [CrossRef]
85. Ekren, S.; Sönmez, Ç.; Özçakal, E.; Kurttaş, Y.S.K.; Bayram, E.; Gürgülü, H. The effect of different irrigation water levels on yield and quality characteristics of purple basil (*Ocimum basilicum* L.). *Agric. Water Manag.* **2012**, *109*, 155–161. [CrossRef]
86. Shields, L.M. Leaf xeromorphy as related to physiological and structural influences. *Bot. Rev.* **1950**, *16*, 399–447. [CrossRef]
87. Liu, H.; Wang, X.; Wang, D.; Zou, Z.; Liang, Z. Effect of drought stress on growth and accumulation of active constituents in *Salvia miltiorrhiza* Bunge. *Ind. Crops Prod.* **2011**, *33*, 84–88. [CrossRef]
88. Lu, X.; Yin, Y.; Yang, M.; Zhang, S.; Niu, Z.; Wu, L.; Chen, C. Effects of Drought Stress on the Growth and Physiological Characteristics of *Idesia polycarpa* Maxim. *Horticulturae* **2025**, *11*, 834. [CrossRef]
89. Hura, T.; Hura, K.; Ostrowska, A. Drought-Stress Induced Physiological and Molecular Changes in Plants. *Int. J. Mol. Sci.* **2022**, *23*, 4698. [CrossRef] [PubMed]
90. Samanta, A.; Das, G.; Das, S.K. Roles of flavonoids in plants. *Int. J. Pharm. Sci. Technol.* **2011**, *6*, 12–35.
91. Caser, M.; Chitarra, W.; D'Angiolillo, F.; Perrone, I.; Demasi, S.; Lovisolo, C.; Pistellie, L.; Pistellid, L.; Scariotet, V. Drought stress adaptation modulates plant secondary metabolite production in *Salvia dolomitica* Codd. *Ind. Crops Prod.* **2019**, *129*, 85–96. [CrossRef]
92. Patil, J.R.; Mhatre, K.J.; Yadav, K.; Yadav, L.S.; Srivastava, S.; Nikalje, G.C. Flavonoids in plant-environment interactions and stress responses. *Discov. Plants* **2024**, *1*, 68. [CrossRef]
93. Singh, M.; Ramesh, S. Effect of irrigation and nitrogen on herbage, oil yield and water-use efficiency in rosemary grown under semi-arid tropical conditions. *J. Med. Aromat. Plant Sci.* **2000**, *22*, 659–662.
94. Baher, Z.F.; Mirza, M.; Ghorbanli, M.; Rezaii, M.B. The influence of water stress on plant height, herbal and essential oil yield and composition in *Satureja hortensis* L. *Flavour Fragr. J.* **2002**, *17*, 275–277. [CrossRef]
95. Bettaieb, I.; Zakhama, N.; Wannes, W.A.; Kchouk, M.E.; Marzouk, B. Water deficit effects on *Salvia officinalis* fatty acids and essential oils composition. *Sci. Hortic.* **2009**, *120*, 271–275. [CrossRef]
96. Austen, N.; Walker, H.J.; Lake, J.A.; Phoenix, G.K.; Cameron, D.D. The regulation of plant secondary metabolism in response to abiotic stress: Interactions between heat shock and elevated CO_2. *Front. Plant Sci.* **2019**, *10*, 1463. [CrossRef] [PubMed]
97. Shomali, A.; Das, S.; Arif, N.; Sarraf, M.; Zahra, N.; Yadav, V.; Aliniaeifard, S.; Chauhan, D.K.; Hasanuzzaman, M. Diverse Physiological Roles of Flavonoids in Plant Environmental Stress Responses and Tolerance. *Plants* **2022**, *11*, 3158. [CrossRef]
98. Ahl, H.S.A.; Sabra, A.; Hegazy, M. Salicylic acid improves growth and essential oil accumulation in two *Nepeta cataria* chemotypes under water stress conditions. *Ital. J. Agrometeorol.* **2013**, *21*, 25–36.
99. Nawaz, H.; Türkay, C.; Karaman, R.; Akgün, I.; Şenyiğit, U. Biochemical response of maize plants to water deficit and *Bacillus simplex* inoculation. *Sci. Rep.* **2026**, *16*, 11016. [CrossRef]
100. Herms, D.A.; Mattson, W.J. The Dilemma of Plants: To Grow or Defend. *Q. Rev. Biol.* **1992**, *67*, 283–335. [CrossRef]
101. Xie, Z.; Kapteyn, J.; Gang, D.R. A systems biology investigation of the MEP/terpenoid and shikimate/phenylpropanoid pathways points to multiple levels of metabolic control in sweet basil glandular trichomes. *Plant J.* **2008**, *54*, 349–361. [CrossRef]
102. Aprotosoaie, A.C.; Gille, E.; Trifan, A.; Vlad Simon, L.; Ancaet, M. Essential oils of Lavandula genus: A systematic review of their chemistry. *Phytochem. Rev.* **2017**, *16*, 761–799. [CrossRef]
103. Bidabadi, S.S.; Vander Weide, J.; Sabbatini, P. Exogenous melatonin improves glutathione content, redox state and increases essential oil production in two Salvia species under drought stress. *Sci. Rep.* **2020**, *10*, 6883. [CrossRef]
104. Farouk, S.; Omar, M.M. Sweet basil growth, physiological and ultrastructural modification, and oxidative defense system under water deficit and silicon forms treatment. *J. Plant Growth Regul.* **2020**, *39*, 1307–1331. [CrossRef]

105. Liao, Z.; Liu, L.; Rennenberg, H.; Du, B. Water deprivation modifies the metabolic profile of lavender (*Lavandula angustifolia* Mill.) leaves. *Physiol. Plant.* **2024**, *176*, e14365. [CrossRef]
106. Gershenzon, J.; Dudareva, N. The function of terpene natural products in the natural world. *Nat. Chem. Biol.* **2007**, *3*, 408–414. [CrossRef] [PubMed]
107. Shah, A.; Smith, D.L. Flavonoids in agriculture: Chemistry and roles in, biotic and abiotic stress responses, and microbial associations. *Agronomy* **2020**, *10*, 1209. [CrossRef]
108. Li, B.; Fan, R.; Sun, G.; Sun, T.; Fan, Y.; Bai, S.; Guo, S.; Huang, S.; Liu, J.; Zhang, H.; et al. Flavonoids improve drought tolerance of maize seedlings by regulating the homeostasis of reactive oxygen species. *Plant Soil* **2021**, *461*, 389–405. [CrossRef]
109. Shabankareh, H.G.; Khorasaninejad, S.; Soltanloo, H.; Shariati, V. Changes in essential oil-content and composition of Lavandula angustifolia 'Hidcote' in response to abscisic acid under irrigation regimes. *Hortic. Plant J.* **2026**, *12*, 460–480. [CrossRef]
110. Nguyen, C.T.T.; Nguyen, N.H.; Choi, W.S.; Lee, J.H.; Cheong, J.J. Biosynthesis of essential oil compounds in *Ocimum tenuiflorum* is induced by abiotic stresses. *Plant Biosyst. Int. J. Deal. All Asp. Plant Biol.* **2022**, *156*, 353–357. [CrossRef]
111. Kalamartzis, I.; Dordas, C.; Georgiou, P.; Menexes, G. The Use of Appropriate Cultivar of Basil (*Ocimum basilicum*) Can Increase Water Use Efficiency under Water Stress. *Agronomy* **2020**, *10*, 70. [CrossRef]
112. Agati, G.; Azzarello, E.; Pollastri, S.; Tattini, M. Flavonoids as antioxidants in plants: Location and functional significance. *Plant Sci.* **2012**, *196*, 67–76. [CrossRef] [PubMed]
113. Dhawan, S.S.; Shukla, P.; Gupta, P.; Lal, R. A cold-tolerant evergreen interspecific hybrid of *Ocimum kilimandscharicum* and *Ocimum basilicum*: Analyzing trichomes and molecular variations. *Protoplasma* **2016**, *253*, 845–855. [CrossRef]
114. Martínez-Natarén, D.A.; Villalobos-Perera, P.A.; Munguía-Rosas, M.A. Morphology and density of glandular trichomes of *Ocimum campechianum* and *Ruellia nudiflora* in contrasting light environments: A scanning electron microscopy study. *Flora* **2018**, *248*, 28–33. [CrossRef]
115. Artemios, M.; Bosabalidis, S.K. Infraspecific variation of leaf anatomy in *Origanum vulgare* grown wild in Greece. *Bot. J. Linn. Soc.* **1997**, *123*, 353–362. [CrossRef]
116. Li, K.; Li, S.J.; Zhou, Z.Y.; Yao, H.Z.; Zhou, Y.; Tang, X.Q.; Wang, K.C. Effects of drought stress on glandular trichomes, stomatal density and volatile exudates of *Schizonepeta tenuifolia*. *Zhongguo Zhongyao Zazhi* **2019**, *44*, 4573–4580. [CrossRef] [PubMed]
117. White, P.J. The pathways of calcium movement to the xylem. *J. Exp. Bot.* **2001**, *52*, 891–899. [CrossRef] [PubMed]
118. Meharg, A. Marschner's Mineral Nutrition of Higher Plants. 3rd edition. P. Marschner Ed.; Amsterdam, Netherlands: Elsevier/Academic Press, 2011; pp. 684, US$124.95. ISBN 978-0-12-384905-2. *Exp. Agric.* **2012**, *48*, 305. [CrossRef]
119. Clemens, S. Molecular mechanisms of plant metal tolerance and homeostasis. *Planta* **2001**, *212*, 475–486. [CrossRef] [PubMed]
120. Chapin, F.S., III. The Mineral Nutrition of Wild Plants. *Annu. Rev. Ecol. Evol. Syst.* **1980**, *11*, 233–260. [CrossRef]